Chaos in the Hill System

By C. Chicone

Department of Mathematics, University of Missouri,
Columbia, MO 65211

B. Mashhoon

Department of Physics and Astronomy, University of Missouri,
Columbia, MO 65211

and D. G. Retzloff

Department of Chemical Engineering, University of Missouri,
Columbia, MO 65211

Abstract.   We define the general Hill system and briefly analyze its dynamical behavior. A particular Hill system representing the interaction of a Keplerian binary system with a normally incident circularly polarized gravitational wave is discussed in detail. In this case, we compute the Poincaré-Melnikov function explicitly and determine its zeros. Moreover, we provide numerical evidence in favor of chaos in this system. The partially averaged equations for the Hill system are used to predict the regular behavior of the Keplerian orbit at resonance with the external radiation.

1   Introduction

In a previous paper on gravitational ionization [1], we discussed — among other things — the long-term dynamical evolution of a Keplerian binary system perturbed by a normally incident *circularly polarized* gravitational wave. If the external radiation is approximated by a monochromatic plane wave, then the dynamical system representing the relative motion of the binary is very similar to the well-known Hill system of celestial mechanics. Moreover, in our numerical work on such a system, there appeared some preliminary evidence in favor of Hamiltonian chaos (see figure 1 of [1]). The purpose of the present work is to extend the notion of a Hill system to include the external perturbation caused by a gravitational wave. The generalized Hill system — which we refer to simply as "the Hill system" due to its close resemblance to the one originally introduced by Hill in his researches on the lunar theory — is presented in section 2. For the sake of simplicity, we then choose a particular case for detailed analysis and discuss its dynamics near resonance in section 3. Moreover, in section 4 the relevant Poincaré-Melnikov function is computed in this case and its countable infinity of zeros are studied. The possible relevance of this infinity of simple zeros to the existence of chaos in the Hill system is discussed. Numerical evidence for such chaos is presented in section 5 and a specific chaotic orbit is described in some detail. In section 6 we turn our attention to the physics of such orbits in the inertial frame in connection with the possible astrophysical relevance of our results. Section 7 is a discussion. Calculational details are relegated to the appendices.

2   The Hill System

Consider a Keplerian binary system under the influence of an external gravitational perturbation. In fact, no binary system in the universe is totally isolated as a consequence of the universality of the gravitational interaction. The binary is generally affected by other masses as well as gravitational radiation. We are interested in a particular form of this interaction that corresponds to Hill's celebrated contribution to the theory of the motion of the Moon [2].

Let us therefore assume that the predominant effect of the external perturbation is a linear tidal force in the equation of *relative* motion, so that this equation can be written as

$$\frac{d^2 X^i}{dt^2} + \frac{k_0 X^i}{r^3} = -K_{ij}(t) X^j, \tag{2.1}$$

where $r = |\mathbf{X}|$, k_0 is a positive constant and $i, j = 1, 2, 3$. Here the tidal matrix $K(t)$ is in general symmetric and traceless. Moreover, we assume that $K_{13} = K_{23} = 0$; indeed, a tidal matrix of this form is consistent with our further requirement that the perturbed relative motion be confined to the (X, Y)-plane. To arrive at the Hill system, we need to restrict the form of $K(t)$ even further; to this end, let us suppose the following general form for K:

$$K_{11} = \xi_0 + \xi_+ \cos \Omega t - \xi_- \sin \Omega t,$$

2

$$K_{12} = \xi_+ \sin \Omega t + \xi_- \cos \Omega t,$$
$$K_{22} = \xi_0 - \xi_+ \cos \Omega t + \xi_- \sin \Omega t,$$
$$K_{33} = -2\xi_0, \tag{2.2}$$

where Ω, ξ_0 and $\xi_\pm$ are real constants.

It is possible to transform the equation of relative motion (2.1) to a rotating coordinate system via $X^i = S_{ij} x^j$, where S is an orthogonal matrix given by

$$S = \begin{bmatrix} \cos\left(\frac{1}{2}\Omega t\right) & -\sin\left(\frac{1}{2}\Omega t\right) & 0 \\ \sin\left(\frac{1}{2}\Omega t\right) & \cos\left(\frac{1}{2}\Omega t\right) & 0 \\ 0 & 0 & 1 \end{bmatrix} \tag{2.3}$$

that represents a rotation by an angle $\frac{1}{2}\Omega t$ about the Z-axis. The equation of relative motion with respect to the rotating frame of reference with coordinates $\mathbf{x} = (x, y, z)$ is then given by the autonomous *Hill system*

$$\frac{d^2 x}{dt^2} - \Omega\frac{dy}{dt} - \frac{1}{4}\Omega^2 x + \frac{k_0 x}{r^3} = -(k_{11}x + k_{12}y),$$
$$\frac{d^2 y}{dt^2} + \Omega\frac{dx}{dt} - \frac{1}{4}\Omega^2 y + \frac{k_0 y}{r^3} = -(k_{21}x + k_{22}y), \tag{2.4}$$

and $z = 0$, where $r = |\mathbf{x}|$ and $k = S^{-1}KS$ is a *constant* matrix given by $k_{11} = \xi_0 + \xi_+$, $k_{12} = \xi_-$, $k_{22} = \xi_0 - \xi_+$, $k_{13} = k_{23} = 0$ and $k_{33} = -2\xi_0$. It is important to note that the sign of Ω has not been specified; in fact, Ω can be positive or negative. In Hill's original system, $\xi_0 = -\Omega^2/8$, $\xi_+ = -3\Omega^2/8$ and $\xi_- = 0$, corresponding to the circular motion of the Earth-Moon system about the Sun with frequency $\Omega/2$. Hill's variational orbit, which is a periodic solution of the Hill system, has played a major role in the lunar theory [3, 4, 5, 6]. In addition to the original system envisaged by Hill, the general case includes a Keplerian binary system that is tidally perturbed by a normally incident circularly polarized gravitational wave [1].

The Hill system may be obtained from the Hamiltonian $H(p_x, p_y, x, y)$,

$$H = \frac{1}{2}p^2 - \frac{k_0}{r} - \frac{1}{2}\Omega L_z + \frac{1}{2}k_{ij}x^i x^j, \tag{2.5}$$

where the canonical momenta are given by $p_x = \dot{x} - \Omega y/2$, $p_y = \dot{y} + \Omega x/2$ and $L_z = xp_y - yp_x$. Here $\dot{x} = dx/dt$ and L_z is the component of relative orbital angular momentum normal to the orbital plane. It is interesting to introduce in this plane polar coordinates (r, θ) such that $x = r\cos\theta$ and $y = r\sin\theta$. Then with respect to the canonical variables $(p_r, p_\theta, r, \theta)$, equation (2.5) can be written as

$$H = \frac{1}{2}\left(p_r^2 + \frac{p_\theta^2}{r^2}\right) - \frac{k_0}{r} - \frac{1}{2}\Omega p_\theta + \frac{1}{2}r^2\left(\xi_0 + \xi_+ \cos 2\theta + \xi_- \sin 2\theta\right), \tag{2.6}$$

where $p_r = \mathbf{x} \cdot \mathbf{p}/r$ and $p_\theta = L_z$. In the absence of the external perturbation, i.e. when Ω, ξ_0 and $\xi_\pm$ vanish, the relative motion of the binary can be described in terms of a Keplerian

ellipse. In the presence of the perturbation, the relative motion in the rotating system of reference can be described at each instant of time in terms of an *osculating ellipse*. That is, if the perturbation is turned off at an instant of time t, the subsequent motion is along the osculating ellipse at t. The energy $E < 0$ and orbital angular momentum $p_\theta > 0$ of the osculating ellipse fix its semimajor axis $a = -k_0/(2E)$ and eccentricity e, $0 \le e < 1$, $p_\theta^2 = a(1-e^2)$. The position on the osculating ellipse at time t is measured from the periastron by the true anomaly v, while the orientation of this whole osculating ellipse is determined in the orbital plane by an angle g such that $\theta = v + g$. The equation of the osculating ellipse is then given by $r = p_\theta^2/(1 + e \cos v) = a(1 - e \cos u)$, where u is the eccentric anomaly. Moreover, $p_r p_\theta = e \sin v$, $(1 - e \cos u) \sin v = (1 - e^2)^{\frac{1}{2}} \sin u$ and the mean anomaly ℓ is given by $\ell = u - e \sin u$. Only positive square roots are considered throughout this paper. The parameters of the osculating ellipse are closely related to Delaunay's action-angle variables. In fact, the Delaunay elements are defined by $L = (k_0 a)^{\frac{1}{2}}$, $G = p_\theta$, ℓ and g for noncircular orbits. It is proved in [5] that the change of variables $(p_r, p_\theta, r, \theta) \to (L, G, \ell, g)$ is canonical. In terms of these planar Delaunay elements, we then have the Hamiltonian for the Hill system in the form

$$H(L, G, \ell, g) = -\frac{k_0^2}{2L^2} - \frac{1}{2}\Omega G + \frac{1}{2}(\xi_0 \mathcal{Q} + \xi_+ \mathcal{C} + \xi_- \mathcal{S}). \tag{2.7}$$

Here $\mathcal{Q} = r^2$ is given by

$$\mathcal{Q}(L, G, \ell, g) = a^2 \left[1 + \frac{3}{2}e^2 - 4\sum_{\nu=1}^{\infty} \frac{\cos \nu\ell}{\nu^2} J_\nu(\nu e) \right], \tag{2.8}$$

and $\mathcal{C} = r^2 \cos 2\theta$ and $\mathcal{S} = r^2 \sin 2\theta$ are given in Delaunay's elements by

$$\mathcal{C} + i\mathcal{S} = a^2 \exp(2ig) \left[\frac{5}{2}e^2 + \sum_{\nu=1}^{\infty} \frac{1}{\nu} \left(K_+^\nu \exp(i\nu\ell) + K_-^\nu \exp(-i\nu\ell) \right) \right], \tag{2.9}$$

where

$$K_\pm^\nu = \frac{1}{2}\nu(A_\nu \pm B_\nu)$$

and

$$A_\nu(e) = \frac{4}{\nu^2 e^2}[2\nu e(1 - e^2)J_\nu'(\nu e) - (2 - e^2)J_\nu(\nu e)], \tag{2.10}$$

$$B_\nu(e) = -\frac{8}{\nu^2 e^2}(1 - e^2)^{\frac{1}{2}}[eJ_\nu'(\nu e) - \nu(1 - e^2)J_\nu(\nu e)]. \tag{2.11}$$

It is interesting to note that $A_\nu = A_{-\nu}$ and $B_\nu = -B_{-\nu}$, so that $K_\pm^{-\nu} = -K_\mp^\nu$.

It follows from our previous work [1] that the Kolmogorov-Arnold-Moser ("KAM") theory is applicable to the general Hill system and that for sufficiently small ξ_0 and $\xi_\pm$ the motion is always bounded. Moreover, our previous work (cf. figure 1 in [1]) indicates the presence of Hamiltonian chaos under certain circumstances. The purpose of the present paper is to investigate further the nature of this chaotic behavior.

4

To simplify the analysis, we will assume in the following that $\xi_0 = 0$ and that $\xi_+ = \epsilon \alpha \Omega^2 \cos \varphi_0$ and $\xi_- = \epsilon \alpha \Omega^2 \sin \varphi_0$. For $\Omega > 0$, this choice of parameters corresponds to the tidal perturbation produced by an incident right circularly polarized (i.e. positive helicity) plane monochromatic gravitational wave of amplitude $\alpha \epsilon$, frequency Ω and phase constant φ_0 propagating along the z-axis. On the other hand, we can let $\Omega \to -\Omega$ in equations (2)–(7) and the resulting system with the same choice of parameters would correspond to left circularly polarized (i.e. negative helicity) radiation of frequency $\Omega > 0$; in this way, our analysis covers both cases of circular polarization. The *transverse* nature of gravitational radiation implies that for this case of normal incidence the binary motion remains planar. The deviation of the curved spacetime metric in the presence of gravitational waves from the flat Minkowski metric is characterized by the perturbation parameter ϵ, $0 < \epsilon \ll 1$. Efforts are under way in several laboratories to detect gravitational waves from astrophysical sources with an expected amplitude of $\epsilon \sim 10^{-20}$. Moreover, the circular polarization amplitude α is such that $|\alpha| \sim 1$. To simplify matters even further, we shall set $\varphi_0 = 0$. The resulting Hill system has been discussed at length in our previous papers [1, 7, 8]. More generally, we have investigated the long-term nonlinear evolution of a Keplerian binary system perturbed by external long-wavelength gravitational waves as well as internal gravitational radiation damping [7, 8, 9, 10]. In fact, gravitational *ionization* provided the original motivation for our analysis [11]. The term "ionization" is derived from a Greek word meaning "to go"; therefore, the concept of ionization need not be restricted to electrically charged systems such as in atomic physics. We have shown that in the case under consideration ionization does not in fact occur for $\epsilon < \epsilon_{\text{kam}}$. This is an important consequence of the KAM theory and implies, on the physical side, that the circularly polarized gravitational wave does not steadily deposit energy into the orbit. Indeed, in the interaction of gravitational waves with a binary system the energy in general flows back and forth between the waves and the binary. Further discussion of gravitational ionization is contained in section 6 in connection with certain large-scale chaotic behavior of the binary orbit for $\epsilon \gtrsim \epsilon_{\text{ch}}$, where ϵ_{ch} corresponds to Chirikov's resonance-overlap condition.

3 Isoenergetic Reduction and Dynamics Near Resonance

With the simplifications already mentioned, the equations of motion derived from the Hamiltonian (2.7) are given by

$$\dot{L} = -\frac{1}{2}\epsilon \alpha \Omega^2 \frac{\partial \mathcal{C}}{\partial \ell},$$
$$\dot{G} = -\frac{1}{2}\epsilon \alpha \Omega^2 \frac{\partial \mathcal{C}}{\partial g},$$
$$\dot{\ell} = \frac{k_0^2}{L^3} + \frac{1}{2}\epsilon \alpha \Omega^2 \frac{\partial \mathcal{C}}{\partial L},$$
$$\dot{g} = -\frac{1}{2}\Omega + \frac{1}{2}\epsilon \alpha \Omega^2 \frac{\partial \mathcal{C}}{\partial G}. \tag{3.1}$$

These equations provide a classic example of a perturbation problem in mechanics. The unperturbed system is expressed in action-angle variables and is completely integrable. We are interested in the dynamics of the perturbed system for small ϵ. This is the "fundamental problem in dynamical systems", according to Poincaré [3].

System (3.1) is a 2-degree-of-freedom autonomous Hamiltonian system. Thus by a well-known method that we will now describe, it can be reduced to a $1\frac{1}{2}$-degree-of-freedom system once the total energy of the system is fixed. Let us describe the reduction technique for the general case. In fact, we will consider the system

$$\dot{q} = \frac{\partial \hat{H}}{\partial p}(q, p, \vartheta, I),$$

$$\dot{\vartheta} = \frac{\partial \hat{H}}{\partial I}(q, p, \vartheta, I),$$

$$\dot{p} = -\frac{\partial \hat{H}}{\partial q}(q, p, \vartheta, I),$$

$$\dot{I} = -\frac{\partial \hat{H}}{\partial \vartheta}(q, p, \vartheta, I), \tag{3.2}$$

where the Hamiltonian function $\hat{H}$ is assumed to be periodic in the angular variable ϑ and there is some region $\mathcal{R}$ of the phase space in which the function $\partial \hat{H}/\partial I$ does not vanish. Under these assumptions, we can solve for I as a function of the remaining variables on an energy surface,

$$\{(q, p, \vartheta, I) : \hat{H}(q, p, \vartheta, I) = h\},$$

to obtain

$$I = \hat{K}(q, p, \vartheta, h).$$

Moreover, because $\partial \hat{H}/\partial I$ does not vanish in $\mathcal{R}$, the variable ϑ is either increasing or decreasing along all orbits in $\mathcal{R}$. Thus, ϑ behaves like a temporal variable and can be taken to be a new independent variable. Indeed, the system

$$\frac{dq}{d\vartheta} = \frac{\partial \hat{H}}{\partial p}\bigg/\frac{\partial \hat{H}}{\partial I}, \quad \frac{dp}{d\vartheta} = -\frac{\partial \hat{H}}{\partial q}\bigg/\frac{\partial \hat{H}}{\partial I} \tag{3.3}$$

is not singular in $\mathcal{R}$. If $\vartheta \mapsto (\hat{u}(\vartheta), \hat{v}(\vartheta))$ is a solution of the system (3.3), then

$$\dot{\vartheta} = \frac{\partial \hat{H}}{\partial I}(\hat{u}(\vartheta), \hat{v}(\vartheta), \vartheta, \hat{K}(\hat{u}(\vartheta), \hat{v}(\vartheta), \vartheta, h)).$$

The solution $t \mapsto \vartheta(t)$ of this scalar differential equation can be used to obtain a solution of the original system (3.2); namely,

$$q(t) = \hat{u}(\vartheta(t)), \quad p(t) = \hat{v}(\vartheta(t)), \quad I(t) = \hat{K}(q(t), p(t), \vartheta(t), h).$$

To obtain a simpler form for the system (3.3), let us use the equation

$$\hat{H}(q, p, \vartheta, \hat{K}(q, p, \vartheta, h)) = h$$

to obtain the identities

$$\frac{\partial \hat{H}}{\partial q} + \frac{\partial \hat{H}}{\partial I}\frac{\partial \hat{K}}{\partial q} = 0, \quad \frac{\partial \hat{H}}{\partial p} + \frac{\partial \hat{H}}{\partial I}\frac{\partial \hat{K}}{\partial p} = 0,$$

and, in turn, system (3.3) in the form

$$\frac{dq}{d\vartheta} = -\frac{\partial \hat{K}}{\partial p}(q, p, \vartheta, h), \quad \frac{dp}{d\vartheta} = \frac{\partial \hat{K}}{\partial q}(q, p, \vartheta, h). \tag{3.4}$$

Under our assumptions, the system (3.4) is periodic in its independent variable. Moreover, system (3.4) is in the form of a "time-dependent" $1\frac{1}{2}$-degree-of-freedom Hamiltonian system with Hamiltonian $-\hat{K}(q, p, \vartheta, h)$. Let us now employ this reduction principle in the study of the system (3.1).

For the Hamiltonian (2.7), we recall that if ϵ is sufficiently small, then the KAM Theorem applies and all orbits in a region $\mathcal{R}$ of an energy surface remain bounded. In particular, if $\mathcal{R}$ is a closed subset of a bounded region, then the function $\partial \mathcal{C}/\partial G$ is bounded over $\mathcal{R}$. Thus, if ϵ is sufficiently small, then $\dot{g} < 0$ along all orbits starting in $\mathcal{R}$. Also, by the Implicit Function Theorem, if the constant energy surface is given by

$$H(L, G, \ell, g) = h,$$

then there is an implicit solution $G = F(L, \ell, g)$ such that

$$H(L, F(L, \ell, g), \ell, g) = h.$$

Using the reduction principle given above, the reduced system in our case is given by

$$\frac{d\ell}{dg} = -\frac{\partial F}{\partial L}(L, \ell, g), \quad \frac{dL}{dg} = \frac{\partial F}{\partial \ell}(L, \ell, g). \tag{3.5}$$

To solve for G in the equation $H(L, G, \ell, g) = h$, let us suppose that in the corresponding equation (2.7) we have $G = G_0 + \epsilon G_1 + O(\epsilon^2)$ and then equate coefficients to obtain the solution up to first order in the small parameter. Let us recall here that the orientation of the background inertial coordinate system is so chosen that $G_0 > 0$ by convention. Our computations yield the values

$$G_0 = -\frac{2}{\Omega}\Big(h_0 + \frac{k_0^2}{2L^2}\Big), \quad G_1 = \alpha \Omega \, \mathcal{C}(L, G_0, \ell, g) - \frac{2}{\Omega}h_1,$$

where h_0 and h_1 are constants such that $h = h_0 + \epsilon h_1$; that is, h_0 is the unperturbed energy in the rotating frame. Thus, we have that

$$\frac{d\ell}{dg} = -\frac{2k_0^2}{\Omega L^3} - \epsilon \alpha \Omega \Big(\frac{\partial \mathcal{C}}{\partial L}(L, G_0, \ell, g) + \frac{2k_0^2}{\Omega L^3}\frac{\partial \mathcal{C}}{\partial G}(L, G_0, \ell, g)\Big) + O(\epsilon^2),$$

$$\frac{dL}{dg} = \epsilon \alpha \Omega \frac{\partial \mathcal{C}}{\partial \ell}(L, G_0, \ell, g) + O(\epsilon^2). \tag{3.6}$$

7

Also, let us note that in view of equation (2.9) the $1\frac{1}{2}$-degree-of-freedom system (3.6) is periodic with period π relative to its independent variable.

The unperturbed system (3.6) is *a priori* stable; that is, it has no hyperbolic orbits. In particular, there are no homoclinic or heteroclinic orbits that can be used to locate transverse homoclinic or heteroclinic points, and, in turn, chaotic invariant sets, after perturbation. Rather, if such transverse homoclinic or heteroclinic points exist in the perturbed system, they must be created directly from the perturbation. As is well known, this fact precludes a direct application of the usual "Melnikov" approach to determine the existence of transverse homoclinic or heteroclinic points. The problem is that the separatrix splitting distance is easily computed to be proportional to $\epsilon M + O(\epsilon^2)$, where M is the Melnikov integral. In the usual case, M is independent of ϵ and thus the first term of the indicated series is the dominant term. However, in the *a priori* stable case, M depends on ϵ and is in fact exponentially small. Therefore, it is not clear if $\epsilon M(\epsilon)$ is the dominant term in the expression for the splitting distance. On the other hand, some rigorous results do exist for systems similar to those that are encountered in the Hill system. Consider, for instance, the rapidly forced pendulum given in the form

$$\ddot{\phi} + \sin\phi = \epsilon^p \sin(\Omega t/\epsilon),$$

where ϵ is a small parameter and p is a positive integer. If $p > 3$, then the Melnikov integral is exponentially small, but the first-order term is still dominant, see [12] and [13].

While the rigorous analysis of the separatrix splitting problem remains unclear at this writing, we will carry through the first-order analysis for Hill's system. Once the rigorous analysis is settled at some future date, we hope that the formulation reported here will prove to be valuable.

To proceed with the perturbation theory for Hill's system, we will use a standard technique: we will "blow up" a resonance and partially average the resulting equations to produce a system, obtained by a change of coordinates, that has homoclinic orbits. We will then compute the Melnikov integral for this system. For a regular perturbation problem where the Melnikov function does not depend on the perturbation parameter, the simple zeros of this function would indicate the presence of chaos in the system. After a blow up at a resonance and a reparametrization of the system to slow time, the Melnikov function does depend on the perturbation parameter. It is for this reason that we are not able to make a rigorous argument that the existence of simple zeros implies that the system is chaotic.

For system (3.6) that is periodic in g with period π, resonance would occur when this period is commensurate with the period of "fast" motion in ℓ, i.e. $\pi\Omega L^3/k_0^2$. Therefore, the resonances are given by relations of the form

$$m\frac{k_0^2}{L^3} = n\Omega$$

where m and n are relatively prime integers. This resonance condition fixes the magnitude of L; therefore, let L_0 denote the resonant value of L at the $(m : n)$ resonance. To blow up

the resonance, we will use the change of coordinates given by

$$L = L_0 + \epsilon^{1/2}\rho, \quad \ell = -\frac{2n}{m}g + \eta.$$

System (3.6), in the new coordinates, has the form

$$\frac{d\rho}{dg} = \epsilon^{1/2}\alpha\Omega\mathcal{C}_\ell + \epsilon\alpha\Omega\rho\big(\mathcal{C}_{\ell L} + \frac{2n}{m}\mathcal{C}_{\ell G}\big) + O(\epsilon^{3/2}),$$

$$\frac{d\eta}{dg} = \epsilon^{1/2}\frac{6n}{mL_0}\rho - \epsilon\Big(\frac{12n}{mL_0^2}\rho^2 + \alpha\Omega(\mathcal{C}_L + \frac{2n}{m}\mathcal{C}_G)\Big) + O(\epsilon^{3/2}), \tag{3.7}$$

where the function $\mathcal{C}$ and its partial derivatives are evaluated at

$$(L_0, G_0(L_0), \eta - 2ng/m, g).$$

For notational convenience, let us define $\mu = \epsilon^{1/2}$ and express the second-order approximation of system (3.7) in the form

$$\frac{d\rho}{dg} = \mu\gamma(\eta, g) + \mu^2\rho\kappa(\eta, g),$$

$$\frac{d\eta}{dg} = \mu c\rho - \mu^2\beta(\rho, \eta, g), \tag{3.8}$$

where c is a constant given by $c = 6n/(mL_0)$ and

$$\gamma(\eta, g) = \alpha\Omega\mathcal{C}_\ell, \qquad \kappa(\eta, g) = \alpha\Omega(\mathcal{C}_{\ell L} + \frac{2n}{m}\mathcal{C}_{\ell G}), \qquad \beta(\rho, \eta, g) = \frac{2c}{L_0}\rho^2 + \alpha\Omega(\mathcal{C}_L + \frac{2n}{m}\mathcal{C}_G).$$

This system is in the correct form for temporal averaging. To this end, we define $\langle\gamma\rangle$ to be the average of γ over the periodic temporal variable g with period $m\pi$ and λ to be the deviation of γ from its mean,

$$\langle\gamma\rangle(\eta) := \frac{1}{m\pi}\int_0^{m\pi}\gamma(\eta, g)\,dg,$$

$$\lambda(\eta, g) := \gamma(\eta, g) - \langle\gamma\rangle(\eta). \tag{3.9}$$

Moreover, let Λ denote the solution of the partial differential equation $\partial\Lambda/\partial g = \lambda$ with the side condition that its average should vanish; that is, $\langle\Lambda\rangle(\eta) = 0$. Using the averaging transformation

$$\rho = \bar\rho + \mu\Lambda(\bar\eta, g), \quad \eta = \bar\eta,$$

system (3.8) takes the form

$$\frac{d\bar\rho}{dg} = \mu\langle\gamma\rangle(\eta) + \mu^2\bar\rho\big(\kappa(\eta, g) - c\frac{\partial\Lambda}{\partial\eta}\big) + O(\mu^3),$$

$$\frac{d\eta}{dg} = \mu c\bar\rho + \mu^2\big(c\Lambda(\eta, g) - \beta(\bar\rho, \eta, g)\big) + O(\mu^3). \tag{3.10}$$

It is useful to introduce dimensionless quantities J and Γ such that

$$\bar\rho = L_0 J, \quad \Lambda = L_0\Gamma;$$

then, the second-order approximation of system (3.10) has the convenient form

$$\frac{dJ}{dg} = \mu \frac{1}{L_0} \langle \gamma \rangle(\eta) + \mu^2 J\Big(\kappa(\eta, g) - \frac{6n}{m}\frac{\partial \Gamma}{\partial \eta}\Big),$$

$$\frac{d\eta}{dg} = 6\frac{n}{m}\mu J + \mu^2\Big(6\frac{n}{m}\Gamma(\eta, g) - \beta(L_0 J, \eta, g)\Big).$$ (3.11)

Recall formula (2.9) and the fact that

$$\gamma = \alpha \Omega \mathcal{C}_\ell\Big(L_0, G_0(L_0), -\frac{2n}{m}g + \eta, g\Big),$$

and note that $\langle \gamma \rangle(\eta)$ is the real part of

$$\frac{1}{m\pi}\int_0^{m\pi} \alpha\Omega\Big(\mathcal{C}_\ell(L_0, G_0(L_0), -\frac{2n}{m}g + \eta, g) + i\mathcal{S}_\ell(L_0, G_0(L_0), -\frac{2n}{m}g + \eta, g)\Big)\, dg$$

$$= i\frac{\alpha\Omega a^2}{m\pi}\int_0^{m\pi} \exp(2ig)\sum_{\nu=1}^{\infty}\Big(K_+^\nu \exp(i\nu\eta - i\frac{2n}{m}\nu g) - K_-^\nu \exp(-i\nu\eta + i\frac{2n}{m}\nu g)\Big)\, dg.$$

This integral vanishes unless $n = 1$ and $m = \nu$, in which case its value is $i\alpha\Omega a^2 K_+^m \exp(im\eta)$. Using the fact that $a = L^2/k_0$, $L = L_0$ at resonance and $\Omega = mk_0^2 L_0^{-3}$, the average of γ at the $(m:1)$ resonance can be written in the form

$$\frac{1}{L_0}\langle \gamma \rangle(\eta) = -\alpha m K_+^m \sin m\eta.$$ (3.12)

If in system (3.11) we substitute using formula (3.12), change to the new angular variable $\sigma := m\eta - \pi$ and the slow temporal variable $\tau := 6\mu g$, then we obtain the equivalent system

$$\frac{d\sigma}{d\tau} = J + \mu\Big[\Gamma\Big(\frac{\sigma + \pi}{m}, \frac{\tau}{6\mu}\Big) - \frac{m}{6}\beta\Big(L_0 J, \frac{\sigma + \pi}{m}, \frac{\tau}{6\mu}\Big)\Big],$$ (3.13)

$$\frac{dJ}{d\tau} = \frac{\alpha m}{6}K_+^m \sin\sigma + \mu J\Big[\frac{1}{6}\kappa\Big(\frac{\sigma + \pi}{m}, \frac{\tau}{6\mu}\Big) - \frac{\partial\Gamma}{\partial\sigma}\Big(\frac{\sigma + \pi}{m}, \frac{\tau}{6\mu}\Big)\Big].$$ (3.14)

Let us note that the unperturbed form of the system (3.13)–(3.14), given by

$$\frac{d\sigma_0}{d\tau} = J_0, \qquad \frac{dJ_0}{d\tau} = -\delta \sin\sigma_0,$$ (3.15)

is the phase-plane system for a mathematical pendulum. Here

$$\delta := -\frac{\alpha m}{6}K_+^m,$$

$m = 1, 2, 3, \ldots$, is the order of the resonance, the constant α could be positive or negative and K_+^m, $2K_+^m = m(A_m + B_m)$ as defined by equations (2.10) and (2.11), is a function of the eccentricity at resonance (e_0). Some properties of $K_\pm^m(e)$ near $e = 0$ and $e = 1$ are given in Appendix A. A graph of the functions $K_\pm^m$ for $m = 1, 2, 3$ is given in figure 1,
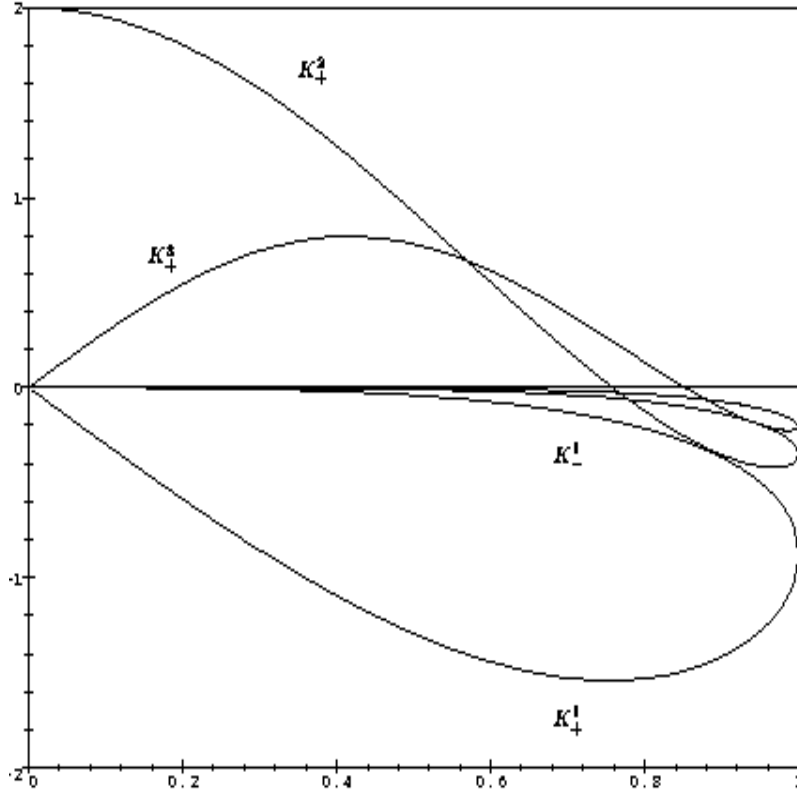
10

Figure 1: Plot of $K_\pm^m$ for $m = 1, 2, 3$. Note that K_+^m and K_-^m meet at $e = 1$. Some of the properties of $K_\pm^m$ are discussed in Appendix A.

which illustrates the analytical results of Appendix A. Our explicit calculations refer to the case of incident positive helicity radiation and hence only K_+^m is involved in the definition of δ (see section 6). It follows from inspection of figure 1 that depending upon the value of the eccentricity e_0, δ could be positive, negative or zero. If $\delta > 0$, then the phase portrait has hyperbolic saddle points at $(J_0, \sigma_0) = (0, \pm\pi)$ that are connected by the heteroclinic solutions

$$\sigma_0(\tau) = 2\arcsin(\tanh(\delta^{1/2}\tau)) = 2\arctan(\sinh(\delta^{1/2}\tau)),$$
$$J_0(\tau) = \pm 2\delta^{1/2}\mathrm{sech}\,(\delta^{1/2}\tau).$$

If $\delta < 0$, then the phase portrait has hyperbolic saddle points at $(J_0, \sigma_0) = (0, 0)$ and $(J_0, \sigma_0) = (0, 2\pi)$ that are connected by the heteroclinic solutions

$$\sigma_0(\tau) = 2\arcsin(\tanh(|\delta|^{1/2}\tau)) + \pi = 4\arctan(\exp(|\delta|^{1/2}\tau)),$$
$$J_0(\tau) = \pm 2|\delta|^{1/2}\mathrm{sech}\,(|\delta|^{1/2}\tau).$$

All of these heteroclinic orbits are also heteroclinic manifolds for the corresponding unperturbed stroboscopic Poincaré map with period $12\pi\mu$. If $\delta = 0$, then the Poincaré-Melnikov approach is not directly applicable; hence, we need to exclude this possibility in the calculation of the Melnikov function. It is therefore clear from the results of Appendix A that all resonant circular orbits ($e_0 = 0$) are excluded from our analysis except for $m = 2$. This

11

is particularly significant in view of a result of *linear* perturbation analysis [11] that the main resonance for a circular orbit occurs for $m = 2$; this is consistent with the reciprocity between the emission and absorption of gravitational radiation. Furthermore, we need to exclude $e_0 \approx 0.76$ for the $(2:1)$ resonance, $e_0 \approx 0.85$ for the $(3:1)$ resonance, etc., since $\delta = 0$ at these zeros of $K_+^m(e)$. Let us remark here that the initial orbit is such that $p_\theta > 0$ by convention; therefore, there is a marked difference between the absorption of positive and negative helicity gravitational waves. In particular, $K_-^m(e)$ does not vanish for $0 < e < 1$. Let us also note here that σ_0 is an odd function of τ while J_0 is an even function; moreover, $J_0 \to 0$ as $\tau \to \pm\infty$. As mentioned previously, we will compute the Melnikov integral along these invariant manifolds. For regular perturbations, the existence of simple zeros for this function implies that, for sufficiently small μ, there are chaotic invariant sets for the perturbed Poincaré map, and hence there are chaotic invariant sets for the perturbed system. In the system (3.13)–(3.14), the perturbation is not regular due to the rapid oscillations of the perturbation when μ is small. Nevertheless, we will compute the Melnikov integral for this system.

4   Poincaré-Melnikov Function

Recall that for a time-periodic planar system of the form

$$\dot{x} = f_0(x, y) + \mu f_1(x, y, t), \quad \dot{y} = g_0(x, y) + \mu g_1(x, y, t),$$

where the unperturbed system is Hamiltonian, if $t \mapsto (x(t), y(t))$ is a solution of the unperturbed system that starts on a heteroclinic or homoclinic orbit, then the Melnikov function defined on this orbit is given by

$$M(\xi) = \int_{-\infty}^{\infty} [f_0(x(t), y(t)) g_1(x(t), y(t), t + \xi) - g_0(x(t), y(t)) f_1(x(t), y(t), t + \xi)] \, dt. \quad (4.1)$$

The computation of M for the system (3.13)–(3.14) is quite complex. However, the end result is reasonably simple. Let us begin with the term $\Gamma = \Lambda/L_0$; as in the computation of formula (3.12), we have that

$$\frac{\gamma}{L_0} = -\alpha m \sum_{\nu=1}^{\infty} \left[K_+^\nu \sin \left(\nu\eta + 2g(1 - \frac{\nu}{m}) \right) + K_-^\nu \sin \left(\nu\eta - 2g(1 + \frac{\nu}{m}) \right) \right]. \quad (4.2)$$

Using formulas (3.12) and (4.2), let us compute

$$\frac{\Lambda}{L_0} = \frac{1}{L_0} \int^g \lambda \, dg = \frac{1}{L_0} \int^g (\gamma - \langle \gamma \rangle) \, dg$$

such that $\langle \Lambda \rangle (\eta) = 0$; in fact, the constant of integration must vanish and the result is

$$\Gamma = \frac{1}{2}\alpha m \left[\sum_{\substack{\nu=1 \\ \nu \neq m}}^{\infty} K_+^\nu \frac{\cos \left(\nu\eta + 2g(1 - \frac{\nu}{m}) \right)}{1 - \frac{\nu}{m}} - \sum_{\nu=1}^{\infty} K_-^\nu \frac{\cos \left(\nu\eta - 2g(1 + \frac{\nu}{m}) \right)}{1 + \frac{\nu}{m}} \right]. \quad (4.3)$$

12

Let us recall that in the definition of the Poincaré-Melnikov function (4.1),

$$f_0 = J_0, \quad f_1 = \Gamma - \frac{m}{6}\beta, \quad g_0 = -\delta \sin \sigma_0, \quad g_1 = J_0\left(\frac{1}{6}\kappa - \frac{\partial\Gamma}{\partial\sigma}\right),$$

where

$$\beta = \frac{12}{m}J_0^2 + \alpha\Omega\left(\mathcal{C}_L + \frac{2}{m}\mathcal{C}_G\right), \quad \kappa = \alpha\Omega\left(\mathcal{C}_{\ell L} + \frac{2}{m}\mathcal{C}_{\ell G}\right).$$

Thus, we have a preliminary expression for the integrand of M (cf. Appendix B)

$$f_0 g_1 - g_0 f_1 = \frac{\alpha\Omega}{6}J_0^2\left(\mathcal{C}_{\ell L} + \frac{2}{m}\mathcal{C}_{\ell G}\right) - J_0^2\frac{\partial\Gamma}{\partial\sigma} + \delta \sin \sigma_0 f_1. \tag{4.4}$$

The Melnikov integral (4.1) is calculated in Appendix B and the result is

$$
\begin{aligned}
M(\xi) = {} & \frac{5}{6}\alpha m^2 H_m I^0 \mathcal{S}^0 \\
& + \frac{1}{2}\alpha m^3 \sum_{\nu=1}^{\infty}\left(\frac{K_+^\nu}{\nu - m}P_\nu^+\mathcal{S}_\nu^+ - \frac{K_-^\nu}{\nu + m}P_\nu^-\mathcal{S}_\nu^-\right) \\
& + \frac{7}{6}\alpha m^2 \sum_{\nu=1}^{\infty}(K_+^\nu P_\nu^+\mathcal{S}_\nu^+ + K_-^\nu P_\nu^-\mathcal{S}_\nu^-) \\
& + \frac{1}{6}\alpha m^2 F_m \sum_{\nu=1}^{\infty}(K_{+e}^\nu P_\nu^+\mathcal{S}_\nu^+ + K_{-e}^\nu P_\nu^-\mathcal{S}_\nu^-). \tag{4.5}
\end{aligned}
$$

Here the only quantities that depend on ξ are $\mathcal{S}^0 = \sin(\xi/3\mu)$ and

$$\mathcal{S}_\nu^\pm = \sin[\pm(\xi/3\mu)(1 \mp \nu/m) + \nu\pi/m],$$

while H_m, F_m, $K_\pm^\nu$ and $K_{\pm e}^\nu = dK_\pm^\nu/de$ all depend upon the eccentricity of the orbit at resonance $e_0 = (1 - \hat{e}_0^2)^{\frac{1}{2}}$, where $\hat{e}_0 = G_0/L_0$. In fact, $F_m = (\hat{e}_0^2 - 2\hat{e}_0/m)/e_0$ and $H_m = e_0(2e_0 + F_m)$. Moreover, I^0 and $P_\nu^\pm$ are also dependent upon e_0 via δ and are given by

$$I^0 = \delta \int_{-\infty}^{\infty} \sin\left(\frac{\tau}{3\mu}\right)\sin\sigma_0(\tau)\, d\tau,$$

$$P_\nu^\pm = \pm\frac{1}{3\mu\nu}\left(1 \mp \frac{\nu}{m}\right)\int_{-\infty}^{\infty} J_0(\tau)\cos\left[\frac{\nu}{m}\sigma_0(\tau) \pm \frac{\tau}{3\mu}\left(1 \mp \frac{\nu}{m}\right)\right]d\tau. \tag{4.6}$$

It is interesting to note that μI^0 and $\mu P_\nu^\pm$ only depend upon $\mu' = \mu|\delta|^{1/2}$. A detailed discussion of these integrals is contained in Appendix B; in fact, a method is described there that can be used to calculate I^0 and $P_\nu^\pm$ whenever $2\nu/m$ is an integer. For instance, it follows from the results of Appendix B that $P_\nu^\pm$ can be explicitly determined for $m = 1, 2$.

It is important to point out that the Poincaré-Melnikov function is periodic with period $6\pi\mu m$ and has a countable infinity of zeros at $\xi_N = 3\mu(1 + mN)\pi$ for any integer N. Indeed, $\mathcal{S}^0$ and $\mathcal{S}_\nu^\pm$ all vanish for $\xi_N/(3\mu) = (1 + mN)\pi$, where $N = 0, \pm1, \pm2, \ldots$; therefore, $M(\xi_N) = 0$.

The zeros of the Melnikov function $M(\xi)$ are all generally expected to be simple. This may be seen from the nature of two consecutive zeros of $M(\xi)$, e.g. ξ_0 and ξ_1, due to the periodicity of the Melnikov integral. However, it is more convenient for our purposes to compute $M'(\xi_N)$ for general N. We note that in the expression (4.5) for $M(\xi)$ only $\mathcal{S}^0$ and $\mathcal{S}_\nu^\pm$ depend upon ξ, and

$$\frac{d\mathcal{S}^0}{d\xi}(\xi_N) = -\frac{1}{3\mu}(-1)^{Nm},$$

$$\frac{d\mathcal{S}_\nu^\pm}{d\xi}(\xi_N) = \mp \frac{1}{3\mu}(-1)^{N(m-\nu)}(1 \mp \frac{\nu}{m}).$$

It follows that

$$-(-1)^{Nm}3\mu M'(\xi_N) = \frac{5}{6}\alpha m^2 H_m I^0 + \frac{2}{3}\alpha m^2 \sum_{\nu=1}^\infty (-1)^{N\nu}(K_+^\nu P_\nu^+ - K_-^\nu P_\nu^-)$$

$$- \frac{7}{6}\alpha m \sum_{\nu=1}^\infty (-1)^{N\nu}\nu(K_+^\nu P_\nu^+ + K_-^\nu P_\nu^-)$$

$$+ \frac{1}{6}\alpha m^2 F_m \sum_{\nu=1}^\infty (-1)^{N\nu}[(1-\frac{\nu}{m})K_{+e}^\nu P_\nu^+ - (1+\frac{\nu}{m})K_{-e}^\nu P_\nu^-], (4.7)$$

assuming that term-by-term differentiation of the infinite series in (4.5) is meaningful.

Inspection of equation (4.7) indicates that in general $M'(\xi_N) \neq 0$. To see this in some detail, let us focus attention on the value of $M'(\xi_N)$ for an eccentricity e_0 such that $0 \leq e_0 \ll 1$. We remark that $\mu^2 M'(\xi_N)$ can be regarded as a function of independent variables e_0 and $\mu' = \mu|\delta|^{1/2}$; in fact, μ' occurs only in I^0 and $P_\nu^\pm$. The forms of $H_m(e)$ and $F_m(e)$ then lead us to distinguish two cases: $m \neq 2$ and $m = 2$. Suppose first that $m \neq 2$; then, the discussion following the introduction of $\delta \neq 0$ in equation (3.15) implies that $e_0 \neq 0$. It follows from the results of Appendix A that the leading term in the expansion of $M'(\xi_N)$ in powers of $e_0 \ll 1$ is

$$\frac{(-1)^{N(m+1)}(m-2)\alpha}{6m\mu e_0}[(m-1)P_1^+ - (m-3)P_3^+],$$

where P_ν^+ is given by equation (4.6). The general form (B.5) given in Appendix B for the integrals in equation (4.6) can be used to show that this leading term is nonzero for $m = 1$; a similar result is expected for $m > 2$. Let us next suppose that $m = 2$. If $e_0 = 0$, then the Melnikov function $M(\xi)$ vanishes in this case; further analysis of this limiting case is beyond the scope of this paper. For $e_0 \neq 0$, the results of Appendix A imply that the leading term in the expansion of $M'(\xi_N)$ in powers of $e_0 \ll 1$ is now

$$\frac{(-1)^N \alpha e_0}{6\mu}(P_1^+ + 25P_3^+),$$

where P_1^+ and P_3^+ are given by equation (4.6) for $m = 2$. The general form (B.5) given in Appendix B for the integrals in equation (4.6) again indicates that this leading term is nonzero. Hence, $M(\xi)$ has in general simple zeros for $0 < e_0 \ll 1$.

5 Numerical Experiments

We now consider the same Hamiltonian as in the calculation of the Poincaré-Melnikov function,

$$H = \frac{1}{2}\Big(p_r^2 + \frac{p_\theta^2}{r^2}\Big) - \frac{k_0}{r} - \frac{1}{2}\Omega p_\theta + \frac{1}{2}\epsilon\alpha\Omega^2 r^2 \cos 2\theta, \tag{5.1}$$

and will demonstrate numerically that this system could be chaotic near a resonance. We first fix an energy surface $H(p_r, p_\theta, r, \theta) = h$ and consider all orbits confined to this energy surface. For instance, choosing an orbit with $(p_r, p_\theta, r, \theta) = (e, 1, 1, 0)$ at $t = 0$ fixes

$$h = \frac{1}{2}(1 + e^2) - k_0 - \frac{\Omega}{2} + \frac{1}{2}\epsilon\alpha\Omega^2.$$

The equations of motion are

$$\frac{dr}{dt} = p_r,$$
$$\frac{d\theta}{dt} = \frac{p_\theta}{r^2} - \frac{\Omega}{2},$$
$$\frac{dp_r}{dt} = \frac{p_\theta^2}{r^3} - \frac{k_0}{r^2} - \epsilon\alpha\Omega^2 r \cos 2\theta,$$
$$\frac{dp_\theta}{dt} = \epsilon\alpha\Omega^2 r^2 \sin 2\theta, \tag{5.2}$$

which can be integrated with different initial conditions all with $H(p_r, p_\theta, r, \theta) = h$. This energy equation can be used to calculate p_θ algebraically in terms of the other variables; we limit our attention here to the solutions of this quadratic equation with $p_\theta > 0$. Moreover, we choose θ as our independent variable and note that the resulting system for (p_r, r) is periodic in θ with period π. We then consider the Poincaré map and plot in the (p_r, r)-plane the result of our numerical integration of the system at $\theta = 0, \pi, 2\pi, \ldots$. In following this procedure, we encounter the difficulty that θ is not necessarily monotonic. Despite this complication, it is possible to obtain useful information from the integration of system (5.2) as in our previous work (see figure 1 of [1]). To avoid this problem altogether, let us restrict attention to those orbits that stay with a simple branch of $p_\theta > 0$. That is, we note that $H(p_r, p_\theta, r, \theta) = h$ has the solution

$$p_\theta = \frac{1}{2}\Omega r^2 [1 \pm (1 - U)^{1/2}],$$

where

$$U = \frac{8}{\Omega^2 r^2}\Big(\frac{1}{2}p_r^2 - \frac{k_0}{r} - h\Big) + 4\epsilon\alpha \cos 2\theta.$$

Thus the system (5.2) reduces to

$$\frac{dr}{dt} = p_r,$$
$$\frac{d\theta}{dt} = \pm\frac{1}{2}\Omega(1 - U)^{1/2},$$
$$\frac{dp_r}{dt} = -\frac{1}{r}p_r^2 + \frac{k_0}{r^2} + \frac{2h}{r} + \frac{1}{2}\Omega^2 r[1 - 4\epsilon\alpha \cos 2\theta \pm (1 - U)^{1/2}], \tag{5.3}$$

15

where the upper (lower) sign corresponds to the positive (negative) branch of $\dot{\theta}$. We have subjected the system (5.3), *restricted to the positive branch of $\dot{\theta}$*, to numerical analysis and have found numerical evidence for Hamiltonian chaos as presented in figure 2.

It is interesting to consider scale transformations in the dynamical systems (5.2) and (5.3) along the lines described in detail in our previous work [8, 9, 10]. The result is that we can use dimensionless quantities and set $k_0 = 1$ once we use the initial semimajor axis of the binary system as our unit of length and the initial period of the binary divided by 2π as our unit of time. We shall use this convention in the numerical experiments reported in this paper.

Partial phase portraits of the Poincaré map for system (5.3) are depicted in figures 2 and 3, where we have chosen the parameter values ($k_0 = 1$)

$$\Omega = 1, \qquad \alpha = 2, \tag{5.4}$$

for the plane right circularly polarized gravitational wave that propagates perpendicularly to the orbital plane. Also, for the top panel of figure 2 the external perturbation is absent so that

$$\epsilon = 0, \qquad h = -0.999982, \tag{5.5}$$

while for the bottom panel of figure 2 and for figure 3

$$\epsilon = 0.0131, \qquad h = -0.986882. \tag{5.6}$$

In these graphs, the horizontal axis corresponds to the variable p_r while the vertical axis corresponds to r. Inspection of the system (5.3) reveals that the phase portrait of the Poincaré map is in general symmetric about the line $p_r = 0$.

The top panel of figure 2 depicts several orbits corresponding to invariant tori for the unperturbed system ($\epsilon = 0$), whereas the bottom panel depicts several orbits for the perturbed system ($\epsilon \neq 0$). Let us note that the stochastic region in figure 2 is obtained as a single orbit. This same orbit is also shown in the top panel of figure 3. It can be obtained via integration of system (5.3), or (5.2), with

$$(r, \theta) = (0.61927711963654, 0)$$

and

$$(p_r, p_\theta) = (0.51405620574951, 0.83454334164660)$$

as the initial conditions and with the parameters given in equations (5.4) and (5.6). This chaotic orbit is near the unperturbed $(1 : 1)$ resonant torus. Let us recall here that the energy of the osculating ellipse is given by

$$E = \frac{1}{2}(p_r^2 + \frac{p_\theta^2}{r^2}) - \frac{k_0}{r}, \tag{5.7}$$

so that the semimajor axis is $a = -k_0/(2E)$ and the corresponding Delaunay element is $L = (k_0 a)^{1/2}$. The $(m : n)$ resonance occurs at $mk_0^2/L_0^3 = n\Omega$; however, in the case under
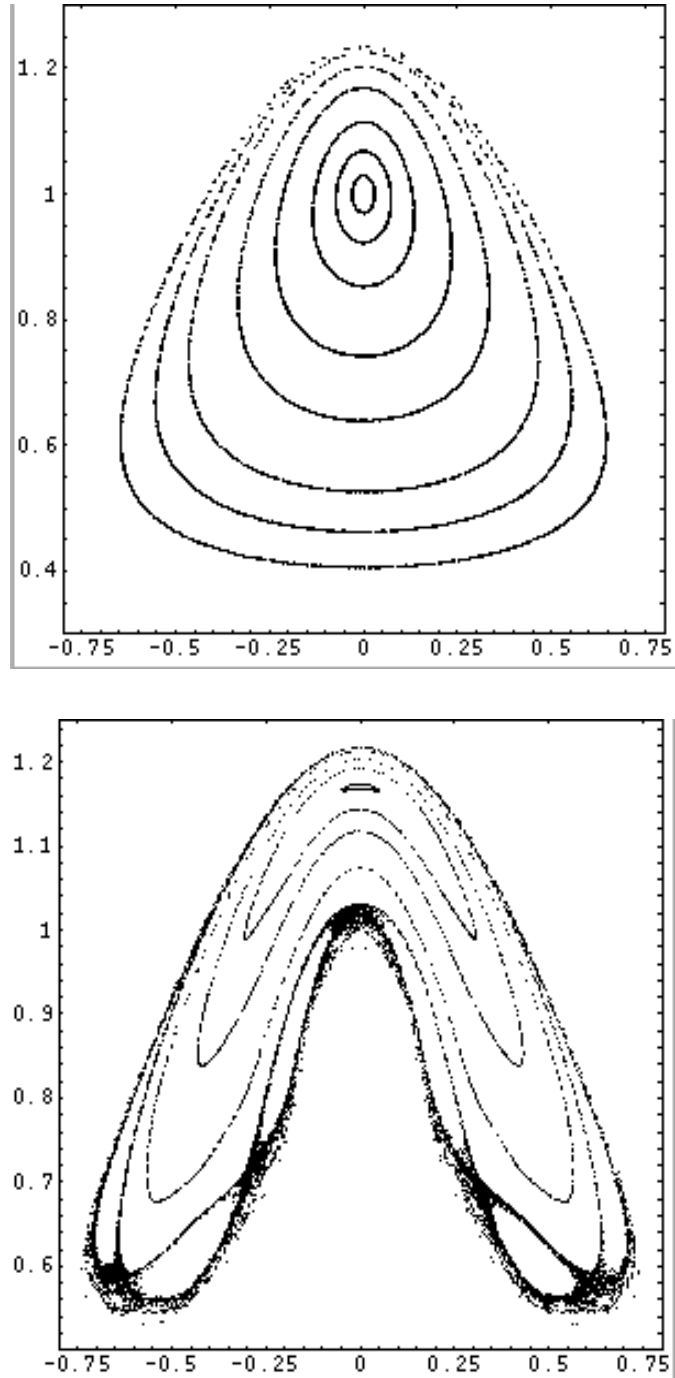
Figure 2: The phase portrait of the Poincaré map for system (5.3) with the parameters given in displays (5.4)–(5.6). The top panel is a phase portrait for the unperturbed system (5.5) while the bottom panel depicts a phase portrait for a perturbed system (5.6) on a nearby energy surface.
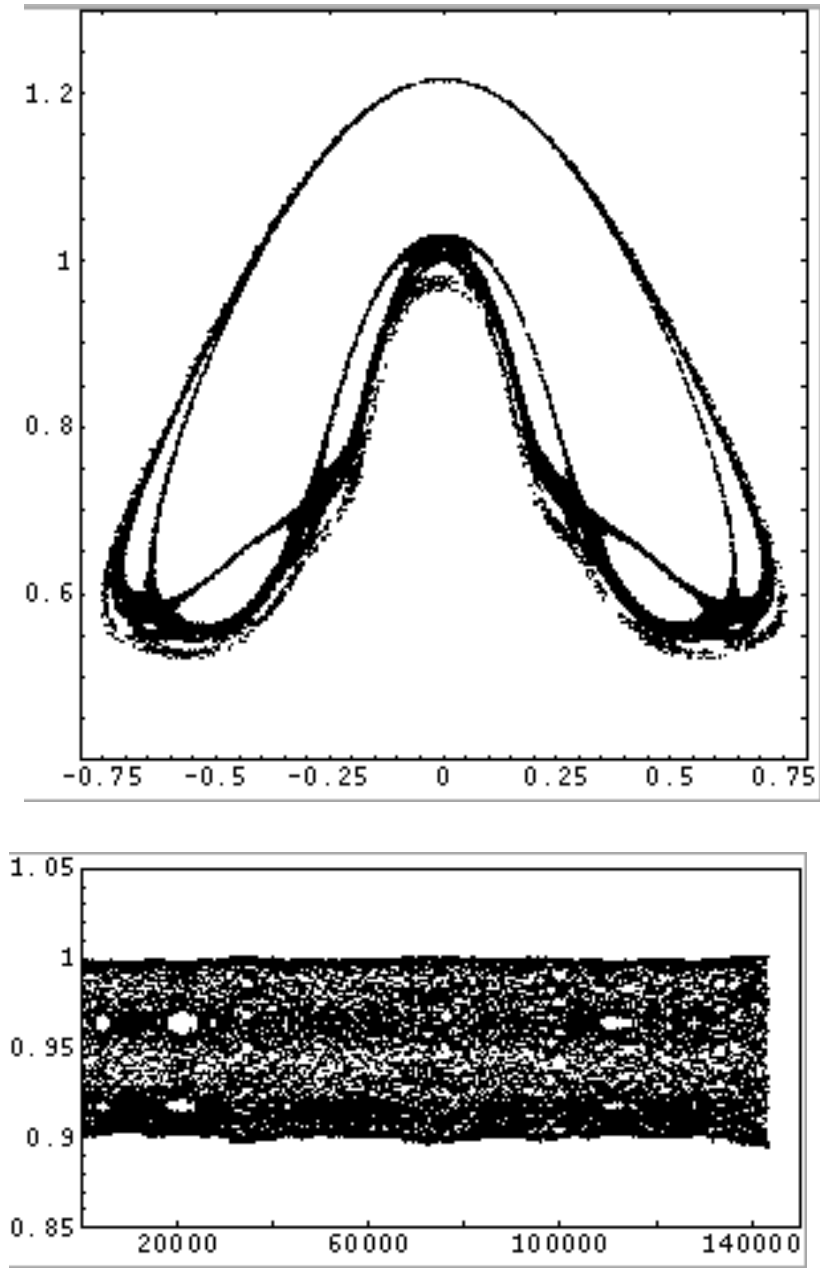
Figure 3: The top panel shows a single orbit of the Poincaré map for system (5.3) with the parameters given in displays (5.4) and (5.6). The bottom panel is a graph of the Delaunay variable L versus time for the same orbit. It follows from this plot that the behavior of the semimajor axis $(a = L^2)$ of the osculating ellipse is *chaotic* in this case.

consideration here the primary resonances are $(m : 1)$ resonances and our chaotic orbit is near the dominant $(1 : 1)$ resonance. Thus L for the chaotic orbit is likely to fluctuate about the $(1 : 1)$ resonant value $L_0 = 1$, though in the case under consideration we expect that secondary $(m : n)$ resonances with $n > 1$ are also involved since ϵ is large enough. The bottom panel of figure 3 is a graph of the Delaunay variable L versus time for the same orbit depicted in the top panel. The stochastic region filled out by the orbit depicted in figure 3, an orbit of a 2-degree-of-freedom time-independent Hamiltonian, seems to be bounded by KAM tori. The fine structure of the graph of L versus t over short time scales, i.e. a few thousand units of time, shows both chaotic and apparently regular oscillations. These are accounted for by reference to the orbit of the corresponding Poincaré map shown in the top panel of figure 3. The corresponding trajectory visits regions near hyperbolic saddle points where transversal crossings of stable and unstable manifolds induce a homoclinic tangle with embedded Smale horseshoes, etc. Thus a sojourn near such a region produces a highly chaotic apparent change in the semimajor axis of the corresponding osculating ellipse. However, when the orbit is "distant" from these hyperbolic saddle points, the semimajor axis of the osculating ellipse oscillates with apparent regularity though the regimes of apparent regularity are dependent on the scale at which the fluctuations in L are observed. This results in a form of Hamiltonian intermittency. Of course, the sojourn time for apparently chaotic (large-amplitude chaotic signal) versus apparently regular (small-amplitude chaotic signal) oscillations is itself highly chaotic in our numerical experiments.

The width of the stochastic layer (δL) in figure 3 may be estimated on the basis of the following considerations: If $\epsilon = 0$, one finds that the variation of $E = h + \Omega p_\theta / 2$ vanishes along the orbit (cf. eq. (5.2)) and hence L is constant $(\delta L/L = 0)$. Physically, this comes about since an ellipse is simply viewed from a rotating frame. Once the perturbation is turned on, the KAM theory implies that for sufficiently small $\epsilon > 0$ the motion is bounded for all time. Inspection of the system (5.3) then reveals that the small parameter in the problem is effectively $4|\alpha|\epsilon$ as $0 \leq |\cos 2\theta| \leq 1$; therefore, we expect that $\delta L/L \approx 4|\alpha|\epsilon$ in agreement with the data of figure 3.

The phase portrait of the Poincaré map for system (5.3) exhibits extreme sensitivity to changes in the parameters of the system. For example, stochastic regions comparable in relative size to the one depicted in figure 3 are not easily detectable for a random choice of parameter values. We have verified all of the main numerical results reported in this paper via two different stiff integration routines using double precision arithmetic. We emphasize that a detailed numerical study of the Hill system is beyond the scope of this paper, since the relevant parameter space is rather large. Our numerical results nevertheless support the view that there is chaos in the Hill system. On the other hand, it would be interesting from an astrophysical standpoint to see the chaotic behavior of the binary in the inertial frame of reference. This issue is taken up in the next section.

6 Inertial Observers and the Hill System

The equation of motion (1) can be derived from the Hamiltonian

$$\mathcal{H} = \frac{1}{2}P^2 - \frac{k_0}{r} + \frac{1}{2}K_{ij}X^i X^j$$

in the inertial frame of reference. This Hamiltonian can be written in polar coordinates (r, Θ) as

$$\mathcal{H} = \frac{1}{2}\Big(P_r^2 + \frac{P_\Theta^2}{r^2}\Big) - \frac{k_0}{r} + \frac{1}{2}r^2[\xi_0 + \xi_+ \cos(2\Theta - \Omega t) + \xi_- \sin(2\Theta - \Omega t)], \qquad (6.1)$$

where we have used equation (2) for the tidal matrix. Let us recall here that Ω can be positive or negative.

The connection between the inertial motion and the Hill motion based on Hamiltonian (2.6) can be simply obtained by referring the inertial motion based on the Hamiltonian (6.1) to the rotating frame. In this process, $\Theta = \theta + \Omega t/2$ and the canonical momenta remain invariant, i.e. $P_r = p_r$ and $P_\Theta = p_\theta$, while the Hamiltonian in the inertial frame is related to that in the rotating frame by the well-known relation

$$\mathcal{H} = H + \frac{1}{2}\Omega p_\theta \qquad (6.2)$$

that expresses angular momentum-rotation coupling. It is important to observe that with the initial conditions $(p_r, p_\theta, r, \theta)$ at $t = 0$ being common to both the inertial and rotating frames, we can integrate the equations of motion in these frames starting from the same initial osculating ellipse.

Let us now choose $\xi_0 = \xi_- = 0$ and $\xi_+ = \epsilon\alpha\Omega^2$ as before. It then follows that the perturbation in the inertial Hamiltonian is of the form $\frac{1}{2}\epsilon\alpha\Omega^2 r^2 \cos(2\Theta \mp \Omega t)$, where the upper (lower) sign stands for plane right (left) circularly polarized gravitational radiation of frequency $\Omega > 0$ that is normally incident on the Keplerian binary system. To describe the *inertial* motion, we introduce the osculating ellipse with semimajor axis $\tilde{a}$, eccentricity $\tilde{e}$, etc., in the inertial frame and the associated Delaunay elements $(\tilde{L}, \tilde{G}, \tilde{\ell}, \tilde{g})$. The equations of motion in terms of Delaunay's variables are

$$\frac{d\tilde{L}}{dt} = \epsilon\frac{\partial\mathcal{H}_{\text{ext}}}{\partial\tilde{\ell}},$$

$$\frac{d\tilde{G}}{dt} = -\epsilon\frac{\partial\mathcal{H}_{\text{ext}}}{\partial\tilde{g}},$$

$$\frac{d\tilde{\ell}}{dt} = \frac{k_0^2}{\tilde{L}^3} + \epsilon\frac{\partial\mathcal{H}_{\text{ext}}}{\partial\tilde{L}},$$

$$\frac{d\tilde{g}}{dt} = \epsilon\frac{\partial\mathcal{H}_{\text{ext}}}{\partial\tilde{G}}, \qquad (6.3)$$

and

$$\frac{d\tilde{\tau}}{dt} = \Omega,$$

where $\tilde{\tau} = \Omega t$ is a new variable and

$$\mathcal{H}_{\text{ext}}(\tilde{L}, \tilde{G}, \tilde{\ell}, \tilde{g}, \tilde{\tau}) = \frac{1}{2}\alpha\Omega^2 r^2 \cos(2\Theta \mp \tilde{\tau}).$$

We are interested in the general behavior of system (6.3) taking into consideration the fact that the motion is always bounded for $\epsilon < \epsilon_{\text{kam}}$ as a consequence of the KAM Theorem.

There are two frequencies in the dynamical system under consideration here, namely the Keplerian frequency $\omega = k_0^2/\tilde{L}^3$ and the frequency of the external radiation Ω; hence, the possibility of resonance cannot be ignored. Thus the averaging principle is in general inapplicable here due to the fact that resonance could occur. Indeed, resonance could come about when ω and Ω are commensurate, i.e. relatively prime integers m and n exist such that $m\omega = n\Omega$; at this $(m:n)$ resonance, $\tilde{L}$ is fixed at its resonant value $\tilde{L}_0$. It will be shown in this section that for system (6.3) the *primary* resonances are in fact $(m:1)$ resonances, i.e. $n = 1$. The resonant behavior of the system around the $(m:1)$ resonance manifold can then be described by the partially averaged equations for system (6.3).

It is important to point out here that the $(m:n)$ resonance is *invariant*, i.e. the resonance is the same whether it is encountered in the rotating frame of reference or in the inertial frame of reference. To make this point explicit, let us note that the energy of the osculating ellipse

$$\mathcal{E} = \frac{1}{2}(P_r^2 + \frac{P_\Theta^2}{r^2}) - \frac{k_0}{r}$$

is an invariant quantity in the sense described above ($\mathcal{E} = E$), and hence so is the semimajor axis of the resonant orbit and its corresponding Delaunay element $\tilde{L} = L = (-k_0^2/2\mathcal{E})^{1/2}$ that becomes fixed at resonance. The same holds for the angular momentum ($\tilde{G} = G$) and the eccentricity ($\tilde{e} = e$) of the *osculating* ellipse; nevertheless, the tildes on the Delaunay action variables will be generally kept in the rest of this section as a reminder that the Hill system is being viewed from the inertial reference frame. Chaos is invariant as well and expected to occur near a resonance; indeed, this point can be illustrated with a single chaotic orbit from the case studied in figure 2. This chaotic orbit that is near a $(1:1)$ resonance is given in figure 3. Further illustration of small-amplitude chaos is contained in figures 4 and 5 described below. Figure 6 illustrates large-amplitude chaos that comes about when primary resonances overlap.

The average behavior of the system around the $(m:1)$ resonance manifold can be obtained from the second-order partially averaged dynamics. To this end, let

$$\tilde{L} = \tilde{L}_0 + \epsilon^{\frac{1}{2}}\mathcal{D}, \quad \tilde{\ell} = \frac{k_0^2 t}{\tilde{L}_0^3} + \Phi,$$

such that the second-order averaged equations *in the inertial frame* are given by [9, 10]

$$\dot{\mathcal{D}} = -\epsilon^{\frac{1}{2}}(-mT_c\sin m\Phi + mT_s\cos m\Phi)$$
$$- \epsilon\mathcal{D}(-m\frac{\partial T_c}{\partial\tilde{L}}\sin m\Phi + m\frac{\partial T_s}{\partial\tilde{L}}\cos m\phi),$$

21

$$\dot{\tilde{G}} = -\epsilon\left(\frac{\partial T_c}{\partial \tilde{g}}\cos m\Phi + \frac{\partial T_s}{\partial \tilde{g}}\sin m\Phi\right),$$

$$\dot{\Phi} = -\epsilon^{\frac{1}{2}}\frac{3k_0^2\mathcal{D}}{\tilde{L}_0^4} + \epsilon\left(\frac{6k_0^2\mathcal{D}^2}{\tilde{L}_0^5} + \frac{\partial T_c}{\partial \tilde{L}}\cos m\Phi + \frac{\partial T_s}{\partial \tilde{L}}\sin m\Phi\right),$$

$$\dot{\tilde{g}} = \epsilon\left(\frac{\partial T_c}{\partial \tilde{G}}\cos m\Phi + \frac{\partial T_s}{\partial \tilde{G}}\sin m\Phi\right). \tag{6.4}$$

Here $T_c = \mathcal{F}_\pm^m(\tilde{L}, \tilde{G})\cos 2\tilde{g}$ and $T_s = \mp\mathcal{F}_\pm^m(\tilde{L}, \tilde{G})\sin 2\tilde{g}$, where

$$\mathcal{F}_\pm^m = \frac{\alpha}{2m}\Omega^2\tilde{a}^2 K_\pm^m(\tilde{e}) \tag{6.5}$$

for $n = 1$. If $n \neq 1$, $T_c = T_s = 0$ and primary resonances do not occur. It follows that for system (6.3) the primary resonances are given by $m\omega = \Omega$. The system (6.4) is evaluated at $\tilde{L} = \tilde{L}_0$.

The second-order averaged dynamics can be simplified if we introduce a new variable $\Delta = m\Phi \pm 2\tilde{g}$. It is then straightforward to recast (6.4) into the form

$$\dot{\mathcal{D}} = m\epsilon^{\frac{1}{2}}(\mathcal{F}_\pm^m + \epsilon^{\frac{1}{2}}\mathcal{D}\mathcal{F}_{\pm\tilde{L}}^m)\sin\Delta,$$

$$\dot{\tilde{G}} = \pm 2\epsilon\mathcal{F}_\pm^m\sin\Delta,$$

$$\dot{\Delta} = -\epsilon^{\frac{1}{2}}\frac{3\Omega}{\tilde{L}_0}\mathcal{D} + \epsilon\frac{6\Omega}{\tilde{L}_0^2}\mathcal{D}^2 + \epsilon(m\mathcal{F}_{\pm\tilde{L}}^m \pm 2\mathcal{F}_{\pm\tilde{G}}^m)\cos\Delta, \tag{6.6}$$

where $\mathcal{F}_{\pm\tilde{L}}^m = \partial\mathcal{F}_\pm^m/\partial\tilde{L}$, etc. Restricting attention to the *first-order* averaged equations in (6.6), we find that this system can be integrated. Thus

$$\tilde{G} - \tilde{G}_0 = \pm\frac{2}{m}(\tilde{L} - \tilde{L}_0), \tag{6.7}$$

where $\tilde{G}_0$ is the orbital angular momentum when the system is exactly at resonance. Moreover,

$$\mathcal{D}^2 = \frac{\alpha m}{3}\tilde{L}_0^2 K_\pm^m(\tilde{e}_0)(\cos\Delta - \cos\Delta_0), \tag{6.8}$$

where Δ_0 and $\tilde{e}_0$ belong to the relative orbit at resonance. It follows from equation (6.8) that $\mathcal{D}$ has oscillatory character and the maximum value of $\mathcal{D}^2$ occurs at either $\Delta = (0, 2\pi, 4\pi, \ldots)$ or $(\pi, 3\pi, 5\pi, \ldots)$ depending upon whether $\alpha K_\pm^m(\tilde{e}_0)$ is positive or negative, respectively. The amplitude of the *total* variation in L is thus given by $\delta L = 2\epsilon^{1/2}\mathcal{D}_{\max}$, where

$$\mathcal{D}_{\max}^2 = \frac{2\alpha m}{3}\tilde{L}_0^2 K_\pm^m(\tilde{e}_0)\sin^2\left(\frac{m}{2}\Phi_0 \pm \tilde{g}_0\right) \tag{6.9}$$

for $\alpha K_\pm^m > 0$, and

$$\mathcal{D}_{\max}^2 = -\frac{2\alpha m}{3}\tilde{L}_0^2 K_\pm^m(\tilde{e}_0)\cos^2\left(\frac{m}{2}\Phi_0 \pm \tilde{g}_0\right) \tag{6.10}$$

for $\alpha K_\pm^m < 0$. Other properties of the motion can be studied as well since Δ varies just like a standard nonlinear pendulum. In addition to these results from the first-order averaged equations, small regular corrections exist that are beyond the scope of this paper and are

due to terms of second order in $\epsilon^{1/2}$ in the averaged equations. Furthermore, certain chaotic effects are also expected near the primary $(m : 1)$ resonance.

These theoretical conclusions may be illustrated by a simple example: Imagine a resonant orbit with $(p_r, p_\theta, r, \theta) = (\tilde{e}, 1, 1, 0)$ at $t = 0$ such that $\tilde{e} = 1/2$, $\tilde{g}_0 = -\pi/2$, $\tilde{u} = \pi/3$, $\tilde{v} = \pi/2$ and hence $\Phi_0 = \pi/3 - 3^{1/2}/4$ for this orbit. We choose $k_0 = 1$, $\epsilon = 10^{-3}$, $\alpha = 2$ and $\Omega = m/\tilde{L}_0^3 = m(3/4)^{3/2}$, so that the orbit is initially in $(m : 1)$ resonance. The results of the numerical integration of this system for $m = 1, 2$ are in good agreement with the predictions of the averaged equations (6.7) and (6.8), since the amplitude of the chaotic motion that is present near the resonance is smaller than, or at most comparable with, the amplitude of resonant motion. This is illustrated for the $(2 : 1)$ resonance in figures 4 and 5 for the incident right and left circularly polarized (RCP and LCP) waves, respectively. It is clear from these results that there is a high-frequency component with dominant frequency $\approx \Omega$ that is at least partly chaotic and is superposed on an *average* regular motion. The net amplitude of this "fast" component can be crudely estimated to be $\delta L/L \approx 0.005$ and $\delta G \approx 2\,\delta L$ regardless of polarization; this is in rough agreement with figures 4 and 5. For the regular motion $\Delta_0/2 = \Phi_0 \pm \tilde{g}_0$; hence, for the RCP case $\Delta_0/2 = -(\pi/6 + 3^{1/2}/4)$ and $K_+^2(0.5) \approx 0.923$ so that using equation (6.9) we find $\delta L \approx 0.094$ in good agreement with the numerical results in figure 4 when the small-amplitude chaotic signal is ignored. Similarly, for the LCP case $\Delta_0/2 = 5\pi/6 - 3^{1/2}/4$, $K_-^2(0.5) \approx -0.009$, and using equation (6.10) we find $\delta L \approx 0.006$ for the amplitude of regular oscillations as in figure 5. It is interesting to note that the amplitude of the "chaotic" signal in L is about the same for RCP and LCP waves. However, the response of the orbit with $p_\theta > 0$ to LCP radiation is smaller by an order of magnitude than its response to RCP radiation; hence, the "chaotic" signal in figure 5 is comparable in amplitude to the regular signal that is consistent with the first-order averaged equations. Thus the chaos that appears in figures 4 and 5 has small amplitude; in fact, to encounter large-amplitude chaos as in figures 2 and 3, it seems from our numerical work that the strength of the perturbation must be larger by at least an order of magnitude. The variation of the angular momentum G is equal to the variation of L for $m = 2$ and in (out of) phase with it for RCP(LCP) waves in accordance with equation (6.7) and in agreement with the numerical data of figures 4 and 5. Furthermore, it is clear from equation (6.6) that the angle Δ satisfies the standard equation for a nonlinear pendulum to first order in $\epsilon^{1/2}$ and the frequency associated with the small-amplitude oscillations of this pendulum is $\tilde{\omega}$ given by

$$\tilde{\omega}^2 = \frac{3}{2}\epsilon m\Omega^2 |\alpha K_\pm^m(\tilde{e}_0)|. \tag{6.11}$$

For the RCP case depicted in figure 4, we find that $2\pi/\tilde{\omega} \approx 65$. The pendulum involved here is nonlinear with amplitude $\Delta_0(\text{RCP})$; therefore, the relevant period of oscillation is longer by about 29% resulting in a predicted period of ≈ 84 in agreement with the period of regular oscillations depicted in figure 4. Similarly, for the LCP case depicted in figure 5, we find from equation (6.11) that the period of small-amplitude oscillations is ≈ 670. The period of regular oscillations can again be calculated for the nonlinear pendulum with amplitude $\Delta_0(\text{LCP})$, and it turns out to be longer by about 10% in this case due to the nonlinearity. Thus the predicted period is ≈ 739, which agrees with the numerical results based on the exact system given in figure 5.
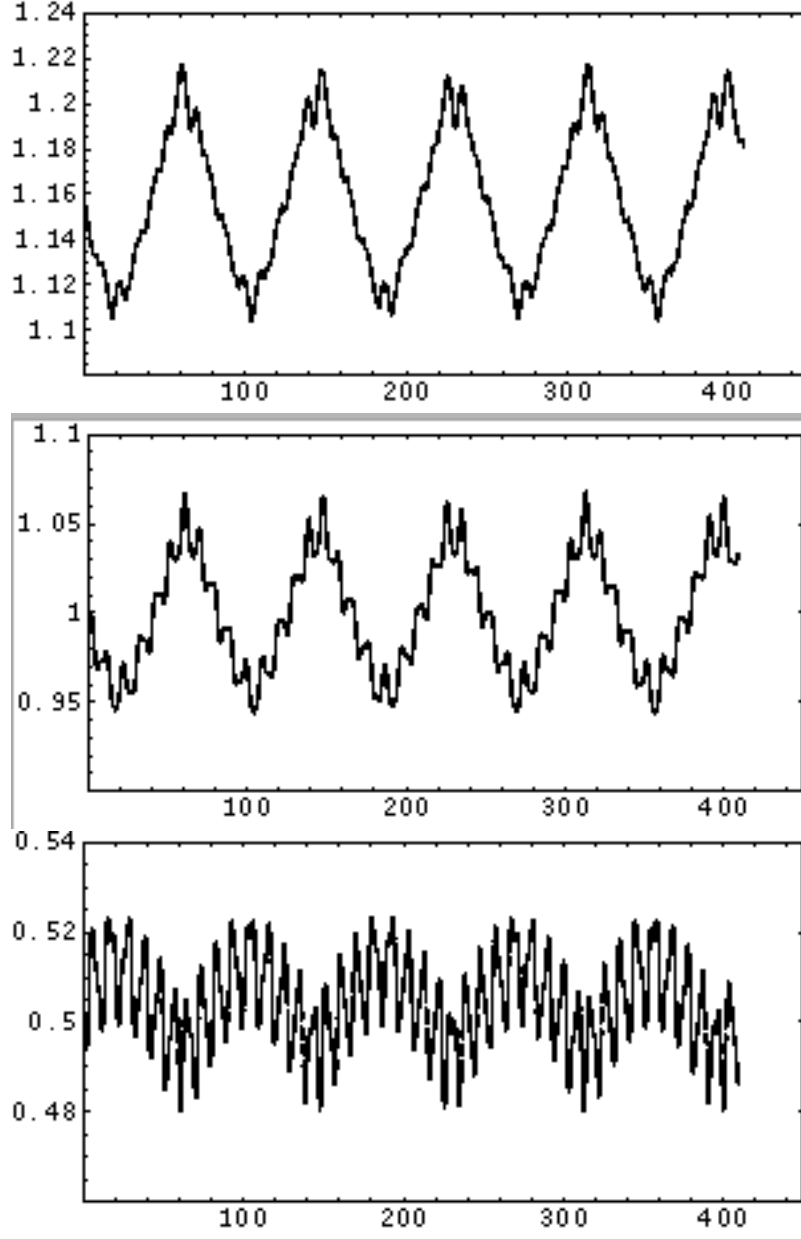
Figure 4: The behavior of relative orbit in a binary system with initial conditions $(p_r, p_\theta, r, \theta) = (0.5, 1, 1, 0)$ in $(2 : 1)$ resonance with a normally incident *right circularly polarized* (RCP) gravitational wave. Here $k_0 = 1$, $\epsilon\alpha = 0.002$ and $\Omega = 2(3/4)^{3/2} \approx 1.299$. The top panel depicts L versus time, the middle panel depicts the angular momentum G versus time and the bottom panel depicts the eccentricity e versus time.
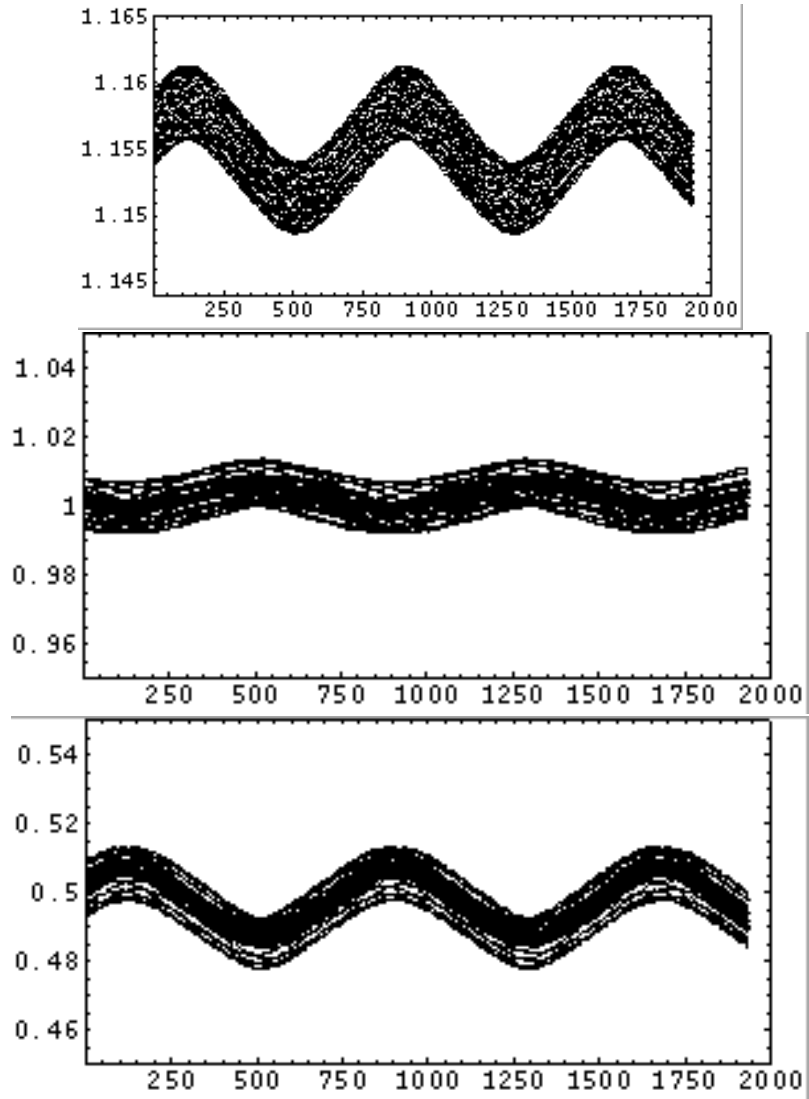
Figure 5: Same as in figure 4, except that the incident radiation is left circularly polarized (LCP).

Large-amplitude chaos near primary resonances can still occur in our system if the Chirikov resonance-overlap condition holds. For instance, numerical experiments with the initial orbit under consideration here indicate the presence of large-scale chaos if the incident RCP wave has frequency $\Omega = \pi/2$. To explain the appearance of large-scale chaos in terms of the Chirikov criterion, let us note that a primary $(m:1)$ resonance would correspond to a Delaunay variable $\tilde{L}_m$ in this case given by $\tilde{L}_m = (2m/\pi)^{1/3}$. Thus the initial Delaunay variable $\tilde{L}$ of the orbit in our example, $\tilde{L}_0 = (4/3)^{1/3} \approx 1.15$, falls between those of $(2:1)$ and $(3:1)$ resonances since $\tilde{L}_2 \approx 1.08$ and $\tilde{L}_3 \approx 1.24$. The Chirikov criterion for large-amplitude chaos [14, 15] can be written in this case as

$$\epsilon_{\text{ch}}^{1/2} = \frac{\tilde{L}_{m+1} - \tilde{L}_m}{[(2m/3)\tilde{L}_m^2|\alpha K_+^m(\tilde{e}_0)|]^{1/2} + [(2(m+1)/3)\tilde{L}_{m+1}^2|\alpha K_+^{m+1}(\tilde{e}_0)|]^{1/2}},$$

using equations (6.9) and (6.10). From $K_+^2(0.5) \approx 0.92$ and $K_+^3(0.5) \approx 0.76$, we find that for $m = 2$,

$$\epsilon_{\text{ch}} \approx 1.65 \times 10^{-3}.$$

Our numerical computations suggest, as is expected, that large-scale chaos occurs for a somewhat smaller choice of the perturbation parameter, certainly for $\epsilon = 10^{-3}$. At much smaller ϵ, for example $\epsilon = 10^{-5}$, the action L still exhibits large-amplitude chaotic effects, but seems to be bounded by KAM tori. However, for $\epsilon \gtrsim \epsilon_{\text{ch}}$ it appears that the action L is no longer confined by KAM tori. This is illustrated in figure 6, where the nature of the binary orbit is studied for $\Omega = \pi/2$ and $\epsilon = 10^{-3}$. At this Chirikov threshold, all KAM tori are expected to disappear and gravitational ionization might take place. It should be noted that in our previous work [7, 8], the ionization process was associated with Arnold diffusion. Here, however, gravitational ionization is due to the fact that $\epsilon > \epsilon_{\text{kam}}$. In figure 6, the perturbed orbit is displayed by plotting $Y = r \sin \Theta$ versus $X = r \cos \Theta$. In the absence of the perturbation, r varies from $\tilde{a}(1-\tilde{e}) = 2/3$ to $\tilde{a}(1+\tilde{e}) = 2$ along the initial elliptical orbit; however, r can reach relatively large values after the RCP perturbation is turned on. In the experiment depicted in figure 6, for instance, the orbit stays generally close to the initial osculating ellipse for about 100000 time units, but large-scale deviations set in eventually such that r can have values as large as ≈ 135 over an interval containing approximately 450000 time units.

As in our previous work on gravitational ionization [1, 7, 8], we find that the binary system is not completely destroyed in the process of gravitational ionization; that is, one member of the binary does not go away once and for all. Rather, the system alternates between dissociation and recombination as in figure 6. This is essentially due to the oscillatory character of the energy exchange between the wave and the relative orbit. In a realistic astrophysical environment, however, new phenomena might lead to the complete ionization of the binary system once one member ventures sufficiently far from the other one.

Finally, let us assume that the system (6.3) is off resonance, i.e. it is far from the primary $(m:1)$ resonance manifold. Then we expect that the motion would involve small amplitude oscillations of frequency $\approx \Omega$ and amplitude $\sim \epsilon$ near the initial osculating ellipse. We have explicitly verified this point for the example given above but with $\Omega = \pi/10$.
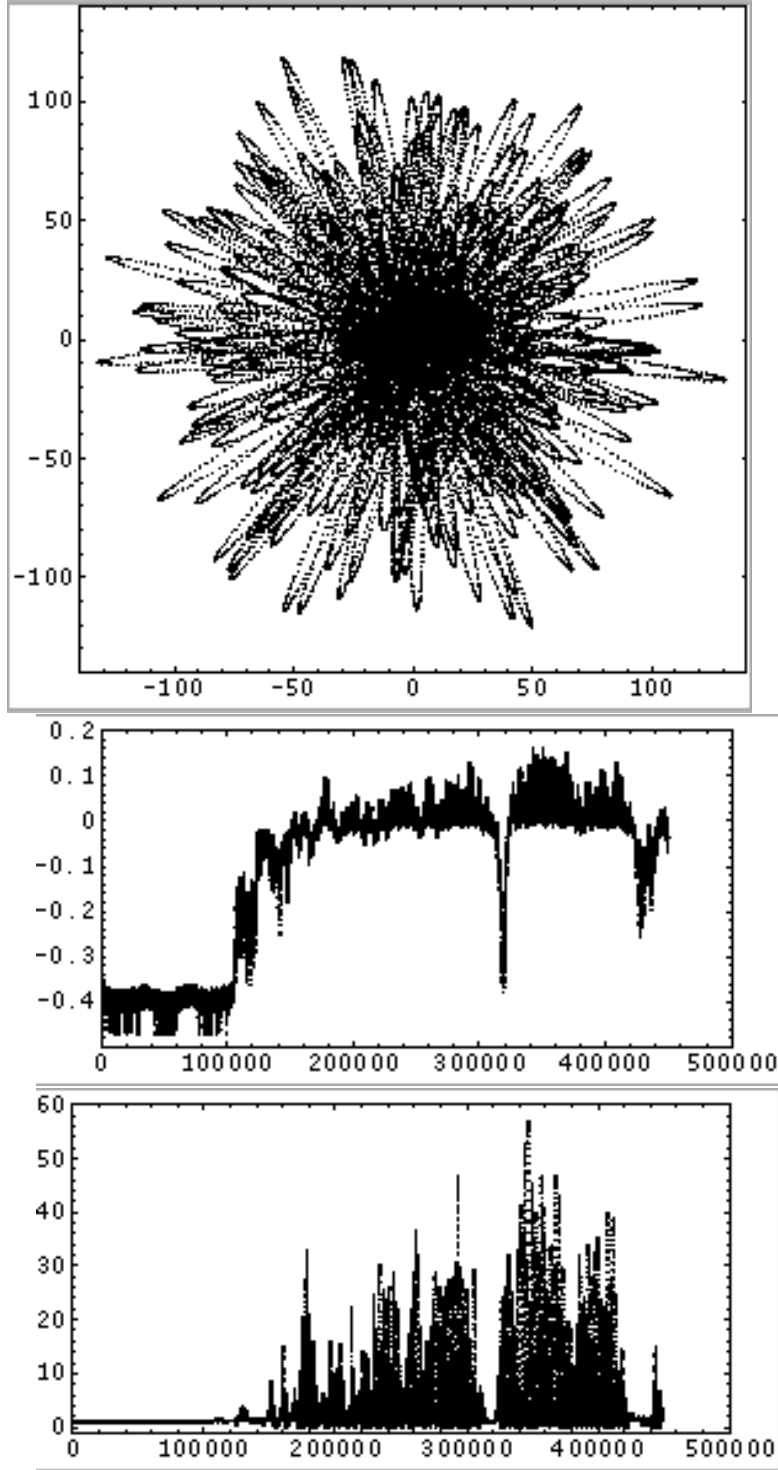
Figure 6: Plot of the perturbed orbit exhibiting large-amplitude chaos. The initial conditions are $(p_r, p_\theta, r, \theta) = (0.5, 1, 1, 0)$ with $k_0 = 1$, and the parameters for a normally incident RCP wave are given by $\epsilon = 10^{-3}$, $\alpha = 2$ and $\Omega = \pi/2$. The top panel depicts a chaotic rosette corresponding to the relative orbit of the binary system over approximately 450000 time units, the middle panel depicts the energy $\mathcal{E} = E$ given by equation (5.7) versus time and the bottom panel depicts the orbital angular momentum $p_\theta = G$ versus time.

27

7   Discussion

The KAM analysis of Hamiltonian chaos is explicitly illustrated in this paper for the interaction of normally incident circularly polarized gravitational radiation with a Keplerian binary system. In the rotating Hill coordinates, the gravitational wave stands completely still and hence the Hill system becomes autonomous. The existence of chaos in this system is demonstrated numerically. On the analytic side, there is no proof at present that the standard approach to Hamiltonian chaos — i.e. the Poincaré-Melnikov theory — is applicable to the Hill system. Nevertheless, the Melnikov function has been useful in this regard in certain analogous circumstances [12, 13]. Therefore, we compute the Melnikov function for the Hill system and show that it has the requisite properties for chaos. The astrophysical implications of these results are explored; in particular, we employ the partially averaged equations to describe the nature of the relative orbit when the binary is at resonance with the incident wave. The possibility of gravitational ionization in the Hill system is discussed in connection with large-scale chaotic orbital motions brought about by incident radiation with an amplitude $\epsilon \gtrsim \epsilon_{\text{ch}}$, where ϵ_{ch} corresponds to Chirikov's resonance-overlap criterion.

A   Some Properties of $K_{\pm}^m(e)$

The quantities

$$K_{\pm}^m(e) := \frac{1}{2}m(A_m \pm B_m), \qquad m = 1, 2, 3, \ldots,$$

can be expressed in terms of Bessel functions via equations (2.10) and (2.11). Using standard expressions for the Bessel functions, we find that for $e \ll 1$,

$$K_{+}^m(e) = \frac{m^{m-2}}{2^{m-3}(m-2)!}e^{m-2} - \frac{(m^2 + 4m - 2)m^{m-1}}{2^{m-1}m!}e^m + O(e^{m+2}). \qquad (\text{A.1})$$

Thus, $K_{+}^1(e) = -3e + O(e^3)$, $K_{+}^2(e) = 2 - 5e^2 + O(e^4)$, $K_{+}^3(e) = 3e + O(e^3)$, etc., for $e \to 0$, so that $K_{+}^m(0) = 2\delta_{m2}$. Moreover, for $e \ll 1$,

$$K_{-}^m(e) = -\frac{(5m + 2)m^{m-1}}{2^{m+1}(m+2)!}e^{m+2} + O(e^{m+4}); \qquad (\text{A.2})$$

hence, $K_{-}^m(0) = 0$. It follows that $K_{-}^m(e) < 0$ on the interval $0 < e < 1$, since we have already shown in [1] that $K_{-}^m(e)$ is monotonically decreasing on this interval (see p. 107 of [1]).

We are also interested in the function $K_{\pm e}^m = dK_{\pm}^m/de$. It is simple to see from (A.1) that $K_{+e}^1(0) = -3$, $K_{+e}^3(0) = 3$, and for all other values of $m \neq 1, 3$, $K_{+e}^m(0) = 0$. Similarly, it follows from (A.2) that $K_{-e}^m(0) = 0$.

For $e \to 1$, one can use the definition of $K_{\pm}^m$ to find

$$K_{\pm}^m(1) = -\frac{2}{m}J_m(m). \qquad (\text{A.3})$$

Here $J_1(1) \approx 0.44$, $J_2(2) \approx 0.35$, etc., and for $m \gg 1$

$$K_\pm^m(1) \sim -\frac{(4/3)^{2/3}}{\Gamma(2/3)} m^{-4/3}. \tag{A.4}$$

It is also interesting to determine the behavior of $K_{\pm e}^m$ as $e \to 1$. We find that $K_{\pm e}^m(1)$ diverges as

$$K_{\pm e}^m(e) \underset{e \to 1}{\sim} \pm (1 - e^2)^{-1/2} \frac{4}{m} J_m'(m), \tag{A.5}$$

which agrees with the results presented in figure 1.

B   Calculation of $M(\xi)$

Let us consider the solution $\tau \mapsto (J_0(\tau), \sigma_0(\tau))$ for the unperturbed heteroclinic orbit of the system (3.15). Starting with equation (4.4), we note that the function $\tau \mapsto \sin \sigma_0(\tau)$ is odd, so only the odd terms in the expression for f_1 contribute to the Melnikov integral. Likewise, the function $\tau \mapsto J_0^2(\tau)$ is even, so only the even terms of $\mathcal{C}_{\ell L} + (2/m)\mathcal{C}_{\ell G}$ and $\partial\Gamma/\partial\sigma$ contribute. To compute β in the formula for f_1, let us consider $\mathcal{C}$ in the form

$$\begin{aligned}
\mathcal{C}(L, G, \ell, g) = {} & \frac{5}{2} \frac{L^4}{k_0^2} \left(1 - \frac{G^2}{L^2}\right) \cos 2g \\
& + \frac{L^4}{k_0^2} \sum_{\nu=1}^{\infty} \frac{1}{\nu} \Big(K_+^\nu \cos(2g + \nu\ell) + K_-^\nu \cos(2g - \nu\ell)\Big),
\end{aligned}$$

and determine its partial derivatives with respect to the action variables

$$\begin{aligned}
\mathcal{C}_L(L, G, \ell, g) = {} & \frac{5L}{k_0^2}(2L^2 - G^2) \cos 2g \\
& + 4\frac{L^3}{k_0^2} \sum_{\nu=1}^{\infty} \frac{1}{\nu} \Big(K_+^\nu \cos(2g + \nu\ell) + K_-^\nu \cos(2g - \nu\ell)\Big) \\
& + \frac{L^4}{k_0^2} \sum_{\nu=1}^{\infty} \frac{1}{\nu} \Big(K_{+L}^\nu \cos(2g + \nu\ell) + K_{-L}^\nu \cos(2g - \nu\ell)\Big)
\end{aligned}$$

and

$$\begin{aligned}
\mathcal{C}_G(L, G, \ell, g) = {} & -5\frac{L^2 G}{k_0^2} \cos 2g \\
& + \frac{L^4}{k_0^2} \sum_{\nu=1}^{\infty} \frac{1}{\nu} \Big(K_{+G}^\nu \cos(2g + \nu\ell) + K_{-G}^\nu \cos(2g - \nu\ell)\Big),
\end{aligned}$$

where $K_{+L}^\nu = \partial K_+^\nu/\partial L$, etc. Also, let us note that here $\ell = (\sigma_0 + \pi - 2g)/m$ and $g = \tau/(6\mu)$. Of course, we must replace τ by $\tau + \xi$ in the Melnikov integrand wherever there is *explicit* dependence upon time in f_1 and g_1. For notational convenience, let us define

$$\zeta_\pm = \frac{\nu}{m}\sigma_0(\tau) \pm \frac{\tau}{3\mu}\left(1 \mp \frac{\nu}{m}\right),$$

$$s_\pm = \pm\frac{\xi}{3\mu}\left(1 \mp \frac{\nu}{m}\right) + \frac{\nu\pi}{m}.$$

We then have an expression for $f_1 = \Gamma - (m/6)\beta$ using equation (4.3),

$$f_1 = \frac{1}{2}\alpha m \sum_{\substack{\nu=1 \\ \nu \neq m}}^{\infty} K_+^\nu \frac{\cos(\zeta_+ + s_+)}{1 - \frac{\nu}{m}} - \frac{1}{2}\alpha m \sum_{\nu=1}^{\infty} K_-^\nu \frac{\cos(\zeta_- + s_-)}{1 + \frac{\nu}{m}}$$

$$- 2J_0^2 - \frac{5}{3}\alpha m^2 \left(1 - \frac{1}{m}\frac{G_0}{L_0} - \frac{1}{2}\frac{G_0^2}{L_0^2}\right)\cos\left(\frac{\tau}{3\mu} + \frac{\xi}{3\mu}\right)$$

$$- \frac{2}{3}\alpha m^2 \sum_{\nu=1}^{\infty} \frac{1}{\nu}\left(K_+^\nu \cos(\zeta_+ + s_+) + K_-^\nu \cos(\zeta_- + s_-)\right)$$

$$- \frac{1}{6}\alpha m^2 L_0 \sum_{\nu=1}^{\infty} \frac{1}{\nu}\left(K_{+L}^\nu \cos(\zeta_+ + s_+) + K_{-L}^\nu \cos(\zeta_- + s_-)\right)$$

$$- \frac{1}{3}\alpha m L_0 \sum_{\nu=1}^{\infty} \frac{1}{\nu}\left(K_{+G} \cos(\zeta_+ + s_+) + K_{-G} \cos(\zeta_- + s_-)\right).$$

Moreover, the odd part of f_1 is given by

$$f_1^{\text{odd}} = -\frac{1}{2}\alpha m \sum_{\substack{\nu=1 \\ \nu \neq m}}^{\infty} K_+^\nu \frac{\sin\zeta_+ \sin s_+}{1 - \frac{\nu}{m}} + \frac{1}{2}\alpha m \sum_{\nu=1}^{\infty} K_-^\nu \frac{\sin\zeta_- \sin s_-}{1 + \frac{\nu}{m}}$$

$$+ \frac{5}{3}\alpha m^2 \left(1 - \frac{1}{m}\frac{G_0}{L_0} - \frac{1}{2}\frac{G_0^2}{L_0^2}\right)\sin\left(\frac{\tau}{3\mu}\right)\sin\left(\frac{\xi}{3\mu}\right)$$

$$+ \frac{2}{3}\alpha m^2 \sum_{\nu=1}^{\infty} \frac{1}{\nu}(K_+^\nu \sin\zeta_+ \sin s_+ + K_-^\nu \sin\zeta_- \sin s_-)$$

$$+ \frac{1}{6}\alpha m^2 L_0 \sum_{\nu=1}^{\infty} \frac{1}{\nu}(K_{+L}^\nu \sin\zeta_+ \sin s_+ + K_{-L}^\nu \sin\zeta_- \sin s_-)$$

$$+ \frac{1}{3}\alpha m L_0 \sum_{\nu=1}^{\infty} \frac{1}{\nu}(K_{+G}^\nu \sin\zeta_+ \sin s_+ + K_{-G}^\nu \sin\zeta_- \sin s_-).$$

On the other hand, only the *even terms* of $\mathcal{C}_{\ell L} + (2/m)\mathcal{C}_{\ell G}$ contribute to M; to compute these terms, we differentiate the expressions for $\mathcal{C}_L$ and $\mathcal{C}_G$ with respect to ℓ,

$$\mathcal{C}_{\ell L} = \frac{4L^3}{k_0^2} \sum_{\nu=1}^{\infty} \left(- K_+^\nu \sin(2g + \nu\ell) + K_-^\nu \sin(2g - \nu\ell)\right)$$

$$+ \frac{L^4}{k_0^2} \sum_{\nu=1}^{\infty} \left(- K_{+L}^\nu \sin(2g + \nu\ell) + K_{-L}^\nu \sin(2g - \nu\ell)\right),$$

$$\mathcal{C}_{\ell G} = \frac{L^4}{k_0^2} \sum_{\nu=1}^{\infty} \left(- K_{+G}^\nu \sin(2g + \nu\ell) + K_{-G}^\nu \sin(2g - \nu\ell)\right).$$

Thus, we find that at resonance

$$\mathcal{C}_{\ell L} + \frac{2}{m}\mathcal{C}_{\ell G} = -\frac{4m}{\Omega} \sum_{\nu=1}^{\infty} \left(K_+^\nu \sin(\zeta_+ + s_+) + K_-^\nu \sin(\zeta_- + s_-)\right)$$

$$- \frac{mL_0}{\Omega} \sum_{\nu=1}^{\infty} \left(K_{+L}^\nu \sin(\zeta_+ + s_+) + K_{-L}^\nu \sin(\zeta_- + s_-)\right)$$

$$- \frac{2L_0}{\Omega} \sum_{\nu=1}^{\infty} \left(K_{+G}^\nu \sin(\zeta_+ + s_+) + K_{-G}^\nu \sin(\zeta_- + s_-)\right)$$

and the even terms are

$$\left(\mathcal{C}_{\ell L} + \frac{2}{m}\mathcal{C}_{\ell G}\right)^{\text{even}} = -\frac{4m}{\Omega} \sum_{\nu=1}^{\infty}(K_+^{\nu}\cos\zeta_+\sin s_+ + K_-^{\nu}\cos\zeta_-\sin s_-)$$

$$-\frac{mL_0}{\Omega}\sum_{\nu=1}^{\infty}(K_{+L}^{\nu}\cos\zeta_+\sin s_+ + K_{-L}^{\nu}\cos\zeta_-\sin s_-)$$

$$-\frac{2L_0}{\Omega}\sum_{\nu=1}^{\infty}(K_{+G}^{\nu}\cos\zeta_+\sin s_+ + K_{-G}^{\nu}\cos\zeta_-\sin s_-).$$

Finally, we must compute $-J_0^2\,\partial\Gamma/\partial\sigma$, where

$$\frac{\partial\Gamma}{\partial\sigma} = -\frac{1}{2}\alpha\left[\sum_{\substack{\nu=1\\\nu\neq m}}^{\infty}\nu K_+^{\nu}\frac{\sin(\zeta_+ + s_+)}{1 - \frac{\nu}{m}} - \sum_{\nu=1}^{\infty}\nu K_-^{\nu}\frac{\sin(\zeta_- + s_-)}{1 + \frac{\nu}{m}}\right]$$

using equation (4.3). Only the even terms in $\partial\Gamma/\partial\sigma$ would contribute to the Melnikov integral, hence

$$\left(\frac{\partial\Gamma}{\partial\sigma}\right)^{\text{even}} = -\frac{1}{2}\alpha\left[\sum_{\substack{\nu=1\\\nu\neq m}}^{\infty}\nu K_+^{\nu}\frac{\cos\zeta_+\sin s_+}{1 - \frac{\nu}{m}} - \sum_{\nu=1}^{\infty}\nu K_-^{\nu}\frac{\cos\zeta_-\sin s_-}{1 + \frac{\nu}{m}}\right].$$

We now have

$$M(\xi) = -\frac{1}{6}\alpha m K_+^m \int_{-\infty}^{\infty}\sin\sigma_0(\tau)f_1^{\text{odd}}\,d\tau + \frac{1}{6}\alpha\Omega\int_{-\infty}^{\infty}J_0^2(\tau)\left(\mathcal{C}_{\ell L} + \frac{2}{m}\mathcal{C}_{\ell G}\right)^{\text{even}}d\tau$$

$$-\int_{-\infty}^{\infty}J_0^2(\tau)\left(\frac{\partial\Gamma}{\partial\sigma_0}\right)^{\text{even}}d\tau.$$

Let us define

$$I^0 := -\frac{1}{6}\alpha m K_+^m \int_{-\infty}^{\infty}\sin\sigma_0(\tau)\sin\left(\frac{\tau}{3\mu}\right)d\tau,$$

$$I_{\nu}^{\pm} := -\frac{1}{6}\alpha m K_+^m \int_{-\infty}^{\infty}\sin\sigma_0(\tau)\sin\zeta_{\pm}\,d\tau,$$

$$\mathcal{S}^0 := \sin\frac{\xi}{3\mu}, \quad \mathcal{S}_{\nu}^{\pm} := \sin s_{\pm},$$

$$J_{\nu}^{\pm} := \int_{-\infty}^{\infty}J_0^2(\tau)\cos\zeta_{\pm}\,d\tau,$$

and note that

$$I_{\nu}^+ = -I_{-\nu}^-, \quad J_{\nu}^+ = J_{-\nu}^-, \quad \mathcal{S}_{\nu}^+ = -\mathcal{S}_{-\nu}^-.$$

It follows that

$$M(\xi) = -\frac{1}{2}\alpha m \sum_{\substack{\nu=1\\\nu\neq m}}^{\infty}\frac{K_+^{\nu}}{1 - \frac{\nu}{m}}I_{\nu}^+\mathcal{S}_{\nu}^+ + \frac{1}{2}\alpha m \sum_{\nu=1}^{\infty}\frac{K_-^{\nu}}{1 + \frac{\nu}{m}}I_{\nu}^-\mathcal{S}_{\nu}^-$$

31

$$+ \frac{5}{3}\alpha m^2 \Big(1 - \frac{1}{m}\frac{G_0}{L_0} - \frac{1}{2}\frac{G_0^2}{L_0^2}\Big) I^0 \mathcal{S}^0$$

$$+ \frac{2}{3}\alpha m^2 \sum_{\nu=1}^{\infty} \frac{1}{\nu}(K_+^\nu I_\nu^+ \mathcal{S}_\nu^+ + K_-^\nu I_\nu^- \mathcal{S}_\nu^-)$$

$$+ \frac{1}{6}\alpha m^2 L_0 \sum_{\nu=1}^{\infty} \frac{1}{\nu}(K_{+L}^\nu I_\nu^+ \mathcal{S}_\nu^+ + K_{-L}^\nu I_\nu^- \mathcal{S}_\nu^-)$$

$$+ \frac{1}{3}\alpha m L_0 \sum_{\nu=1}^{\infty} \frac{1}{\nu}(K_{+G}^\nu I_\nu^+ \mathcal{S}_\nu^+ + K_{-G}^\nu I_\nu^- \mathcal{S}_\nu^-)$$

$$- \frac{2}{3}\alpha m \sum_{\nu=1}^{\infty}(K_+^\nu J_\nu^+ \mathcal{S}_\nu^+ + K_-^\nu J_\nu^- \mathcal{S}_\nu^-)$$

$$- \frac{1}{6}\alpha m L_0 \sum_{\nu=1}^{\infty}(K_{+L}^\nu J_\nu^+ \mathcal{S}_\nu^+ + K_{-L}^\nu J_\nu^- \mathcal{S}_\nu^-)$$

$$- \frac{1}{3}\alpha L_0 \sum_{\nu=1}^{\infty}(K_{+G}^\nu J_\nu^+ \mathcal{S}_\nu^+ + K_{-G}^\nu J_\nu^- \mathcal{S}_\nu^-)$$

$$+ \frac{1}{2}\alpha \sum_{\substack{\nu=1 \\ \nu \neq m}}^{\infty} \frac{\nu K_+^\nu}{1 - \frac{\nu}{m}} J_\nu^+ \mathcal{S}_\nu^+ - \frac{1}{2}\alpha \sum_{\nu=1}^{\infty} \frac{\nu K_-^\nu}{1 + \frac{\nu}{m}} J_\nu^- \mathcal{S}_\nu^-. \tag{B.1}$$

Furthermore, let us define

$$K_{\pm G}^\nu = \frac{\partial e}{\partial G}\frac{d}{de}K_\pm^\nu := \frac{\partial e}{\partial G}K_{\pm e}^\nu,$$

$$K_{\pm L}^\nu = \frac{\partial e}{\partial L}\frac{d}{de}K_\pm^\nu := \frac{\partial e}{\partial L}K_{\pm e}^\nu,$$

$$F_m(e) := L_0\Big(\frac{\partial e}{\partial L} + \frac{2}{m}\frac{\partial e}{\partial G}\Big)\Big|_{(L_0, G_0)}.$$

We recall that $e^2 = 1 - G^2/L^2$; hence,

$$e\frac{\partial e}{\partial L} = \frac{G^2}{L^3}, \quad e\frac{\partial e}{\partial G} = -\frac{G}{L^2},$$

so that

$$\frac{\partial e}{\partial L} = \frac{1}{eL}(1 - e^2), \quad \frac{\partial e}{\partial G} = -\frac{1}{eL}(1 - e^2)^{1/2},$$

and thus

$$F_m(e) = \frac{1}{e}\left[1 - e^2 - \frac{2}{m}(1 - e^2)^{1/2}\right].$$

Moreover, it is useful to define

$$H_m(e) := 1 + e^2 - \frac{2}{m}(1 - e^2)^{1/2},$$

so that

$$H_m(e) - eF_m(e) = 2e^2.$$

32

Finally, let us define

$$P_\nu^\pm := \frac{1}{\nu} I_\nu^\pm - \frac{1}{m} J_\nu^\pm.$$

After collecting terms in equation (B.1) and using the definitions given above, we have an expression for the Melnikov function:

$$
\begin{aligned}
M(\xi) = {}& \frac{5}{6} \alpha m^2 H_m(e) I^0 \mathcal{S}^0 \\
& - \frac{1}{2} \alpha m \sum_{\substack{\nu=1 \\ \nu \neq m}}^{\infty} \frac{\nu K_+^\nu}{1 - \frac{\nu}{m}} P_\nu^+ \mathcal{S}_\nu^+ + \frac{1}{2} \alpha m \sum_{\nu=1}^{\infty} \frac{\nu K_-^\nu}{1 + \frac{\nu}{m}} P_\nu^- \mathcal{S}_\nu^- \\
& + \frac{2}{3} \alpha m^2 \sum_{\nu=1}^{\infty} (K_+^\nu P_\nu^+ \mathcal{S}_\nu^+ + K_-^\nu P_\nu^- \mathcal{S}_\nu^-) \\
& + \frac{1}{6} \alpha m^2 F_m(e) \sum_{\nu=1}^{\infty} (K_{+e}^\nu P_\nu^+ \mathcal{S}_\nu^+ + K_{-e}^\nu P_\nu^- \mathcal{S}_\nu^-).
\end{aligned}
\tag{B.2}
$$

Let us note that in this expression $s_+(\nu = m) = \pi$ so that $\mathcal{S}_m^+ = 0$. Furthermore, we have from the definition of $I_\nu^\pm$ and the fact that $\delta \sin \sigma_0(\tau) = -dJ_0/d\tau$,

$$I_\nu^\pm = \int_{-\infty}^{\infty} -\frac{dJ_0}{d\tau} \sin \zeta_\pm d\tau = \int_{-\infty}^{\infty} J_0 \left[\frac{\nu}{m} J_0 \pm \frac{1}{3\mu} \left(1 \mp \frac{\nu}{m} \right) \right] \cos \zeta_\pm \, d\tau,$$

via integration by parts ($J_0 \to 0$ as $\tau \to \pm\infty$). It thus follows that $P_\nu^\pm = \nu^{-1} I_\nu^\pm - m^{-1} J_\nu^\pm$ is given by equation (4.6). It is interesting to note that in the formula for $M(\xi)$, $P_m^+ = 0$; moreover, the quantity

$$\frac{P_\nu^\pm}{1 \mp \nu/m} = \pm \frac{1}{3\nu\mu} \int_{-\infty}^{\infty} J_0(\tau) \cos \zeta_\pm \, d\tau \tag{B.3}$$

is well defined even for $\nu = m$. In fact, we find from equation (3.15) that

$$\lim_{\nu \to m} \frac{P_\nu^+}{1 - \nu/m} = \frac{1}{3m\mu} \int_{-\infty}^{\infty} J_0(\tau) \cos \sigma_0 \, d\tau = 0.$$

Using these results in equation (B.2), we recover equation (4.5) for $M(\xi)$.

The function $M(\xi)$ refers to a resonance between a Keplerian orbit and an incident circularly polarized wave. Therefore, $M(\xi)$ depends upon the wave amplitude α, the order of the resonance m, the orbital eccentricity at resonance e_0 and the perturbation parameter μ. The explicit form of $M(\xi)$ involves certain combinations of the Bessel functions (i.e. $K_\pm^\nu$ and $K_{\pm e}^\nu$) that depend only on the eccentricity and the integrals in I^0 and $P_\nu^\pm$. The complete evaluation of $P_\nu^\pm$ is beyond the scope of this work; however, $P_\nu^\pm$ can be computed using contour integration when $2\nu/m$ is an integer. To see this, let us assume that $\delta = -(\alpha m/6) K_+^m(e_0) > 0$ and choose the principal branch of $\sigma_0(\tau)$ in the following. Hence the integral in $P_\nu^\pm$ takes the form

$$\mathcal{I}_{jw} = 2 \int_{-\infty}^{\infty} \operatorname{sech}(x) \cos[j \arcsin(\tanh x) + wx] \, dx, \tag{B.4}$$

33

where $j = 2\nu/m$ and $w = \pm(1 \mp \nu/m)/(3\mu\delta^{1/2})$. For the analytic extension of the integrand to the complex plane, it is essential to rewrite the integral in the form

$$\mathcal{I}_{jw} = \int_{-\infty}^{\infty} (\operatorname{sech} x)^{j+1} [(1 + i \sinh x)^j \exp(iwx) + (1 - i \sinh x)^j \exp(-iwx)] \, dx,$$

that is appropriate for the principal branch of σ_0 under consideration here. We note that the integrand is an even function. Let us now imagine a rectangular contour in the complex (x, y)-plane that is symmetric about the y-axis with the two long (eventually infinite) sides parallel to the x-axis at $y = 0$ and $y = 2\pi$. The singularities of the integrand within this contour occur at $i\pi/2$ and $3i\pi/2$. These are poles once j is a positive integer. In this case, a standard application of the Cauchy Theorem for this contour results in

$$[1 - \cosh(2\pi w)] \, \mathcal{I}_{jw} = 2\pi i \, [\text{residue } (i\pi/2) + \text{residue } (3i\pi/2)],$$

where the symmetry of the integrand has been taken into account. The calculation of the residues for arbitrary j is straightforward, but will not be attempted here; however, it is possible to show that $\mathcal{I}_{jw}$ has the general form

$$\mathcal{I}_{jw} = 4\pi w \frac{\exp(-\pi w/2)}{\sinh(\pi w)} W_j(w), \tag{B.5}$$

where $W_j(w)$ is a polynomial in w of degree $j - 1$ such that $jW_j(0)$ vanishes for even j and is equal to $(-1)^{(j-1)/2}$ for odd j. We find that $W_1(w) = 1$, $W_2(w) = -w$, $W_3(w) = (-1 + 2w^2)/3$, etc. Note that $\mathcal{I}_{jw}$ is well defined for $w \to 0$. Moreover, I^0 can also be computed using the approach outlined above. We find that

$$\int_{-\infty}^{\infty} \sin(w_0 x) \sin \sigma_0(x) \, dx = \frac{2\pi w_0}{\cosh(\pi w_0/2)}$$

for the principal branch of σ_0. For I^0, $w_0 = 1/(3\mu\delta^{1/2})$; hence,

$$I^0 = \frac{2\pi}{3\mu \cosh[\pi/(6\mu\delta^{1/2})]}. \tag{B.6}$$

References

[1] C. Chicone, B. Mashhoon and D. G. Retzloff, Gravitational ionization: periodic orbits of binary systems perturbed by gravitational radiation, *Ann. Inst. H. Poincaré, Phys. Théor.*, **64**, 1996, pp. 87–125.

[2] G. Hill, Researches in lunar theory, *Amer. J. Math.*, **1**, 1878, pp. 5-26, 129-147, 245-260.

[3] H. Poincaré, Les Méthodes Nouvelles de la Mécanique Céleste, Vols. **1-3**, *Gauthier-Villars,* Paris, 1892-99.

[4] J. Kovalevsky, Introduction to Celestial Mechanics, *Astrophysics and Space Science Library,* Vol. **7**, Springer-Verlag, 1967.

[5] S. Sternberg, Celestial Mechanics, Vols. **1-2**, W.A. Benjamin, Inc., New York, 1969.

[6] M. C. Gutzwiller, Moon-Earth-Sun: The oldest three-body problem, *Rev. Mod. Phys.,* **70**, 1998, pp. 589–639.

[7] C. Chicone, B. Mashhoon and D. G. Retzloff, On the ionization of a Keplerian binary system by periodic gravitational radiation, *J. Math. Phys.,* **37**, 1996, pp. 3997–4016; Addendum *ibid.* **38**, 1997, p. 544.

[8] C. Chicone, B. Mashhoon and D. G. Retzloff, Gravitational ionization: a chaotic net in the Kepler system, *Class. Quantum Grav.,* **14**, 1997, pp. 699–723.

[9] C. Chicone, B. Mashhoon and D. G. Retzloff, Evolutionary dynamics while trapped in resonance: a Keplerian binary system perturbed by gravitational radiation, *Class. Quantum Grav.,* **14**, 1997, pp. 1831–1850.

[10] C. Chicone, B. Mashhoon and D. G. Retzloff, Chaos in the Kepler System, *Class. Quantum Grav.,* **16**, 1999, pp. 507–527. E-print: http://xxx.lanl.gov/abs/gr-qc/9806107

[11] B. Mashhoon, On tidal resonance, *Astrophys. J.,* **223**, 1978, pp. 285–298;
B. Mashhoon, Tidal radiation, *Astrophys. J.,* **216**, 1977, pp. 591–609;
B. Mashhoon, On the detection of gravitational radiation by the Doppler tracking of spacecraft, *Astrophys. J.,* **227**, 1979, pp. 1019–1036;
B. Mashhoon, Absorption of gravitational radiation, *GRG Abstracts (Jena Meeting),* 1980, pp. 1505-1507;
B. Mashhoon, B. J. Carr and B. L. Hu, The influence of cosmological gravitational waves on a Newtonian binary system, *Astrophys. J.,* **246**, 1981, pp. 569–591.

[12] A. Delshams and T. M. Seara, Splitting of separatrices in Hamiltonian systems with one and a half degrees of freedom, *Math. Phys. Elec. J.,* Vol. **3**, Paper 4, 1997.

[13] J. A. Ellison, M. Kummer and A. W. Sáenz, Transcendentally small transversality in the rapidly forced pendulum, *J. Dynamics Differential Equations,* **5**, no. 2, 1993, pp. 241–277.

[14] B. V. Chirikov, A universal instability of many-dimensional oscillator systems, *Phys. Rep.,* **52**, 1979, pp. 262–379.

[15] A. J. Lichtenberg and M. A. Lieberman, *Regular and Chaotic Dynamics,* 2nd Ed., Springer-Verlag, New York, 1992.